Global Natural Rates in the Long Run: Postwar Macro Trends and the Market-Implied r^* in 10 Advanced Economies[★]

Josh Davis[†] Cristian Fuenzalida[‡] Leon Huetsch[§]
Benjamin Mills[¶] Alan M. Taylor[✠]

June 2023

PRELIMINARY

Prepared for the NBER ISOM Conference in Ispra, Italy, 22–23 June 2023

Abstract

Benchmark finance and macroeconomic models deliver conflicting estimates of the natural rate and bond risk premia. This *natural rate puzzle* applies not only in the U.S. but across many advanced economies. We estimate a unified no-arbitrage macro-finance model with long-run trend factors to obtain a *market-implied natural rate* r^*. Our monthly natural rate estimates cover 10 advanced economies for most of the postwar period, extending coverage over a longer and wider sample than previous studies, and drawing on new sources to construct bond yield curves and excess returns. Our model improves the explanatory power of yield regressions and return forecasts, in and out of sample. Most variation in yields is due to the macro trends r^* and π^*, and not bond risk premia. Our r^* differs from other estimates, and is typically lower, intensifying concerns about secular stagnation and the effective lower-bound. Our estimates covary with growth and demographic variables in a manner consistent with theory and previous findings.

Keywords: bond risk premia, natural rate of interest, inflation expectations, term structure, affine models

JEL classification codes: C13, C32, E43, E44, E47, G12

[★]We thank Ben Bernanke, Joachim Fels, and participants in seminars at the Federal Reserve Bank of San Francisco and Stanford University for helpful discussions. All errors are ours.

[†]PIMCO. Email: josh.davis@pimco.com.

[‡]Graham Capital Management. Email: cristian.fuenzalida@nyu.edu.

[§]University of Pennsylvania. Email: lhuetsch@sas.upenn.edu.

[¶]PIMCO. Email: ben.mills@pimco.com.

[✠]Columbia University; PIMCO; NBER; and CEPR. Email: amt2314@columbia.edu; alan.taylor@pimco.com.

1. Introduction

Like two trains running on different railroads, studies of the natural rate and bond risk premia in the macroeconomic and finance literatures have tended to follow their own line even if ostensibly headed for the same place. The destination is clear and important: rates of interest, across all maturities, matter for saving, investment, capital allocation, economic growth, and monetary policy. But passengers on each route see different landscapes for the most part: on the macro track, a wide focus on slow-moving trends in natural rate Wicksellian models where the fundamental secular driver ties into the rate of output growth with no financial market structure (e.g, Holston, Laubach, and Williams, 2017; Rachel and Summers, 2019; Jordà and Taylor, 2019); on the finance track, a tightly-framed look at cross-section no-arbitrage models of yields and no role for macroeconomic growth (e.g, Litterman and Scheinkman, 1991; Piazzesi, 2010; Adrian, Crump, and Moench, 2013).

But the two tracks converge and a collision was unavoidable. As we show, workhorse finance models generate an implied path for the natural rate dramatically at odds with the macro literature. Equivalently, workhorse macro models generate an implied path for bond risk premia equally at odds with the finance literature. We call this the *natural rate puzzle*. To get on the same track, the two approaches must be somehow shunted together. A consensus unified model should not fail these consistency tests and this is a first-order challenge for macro-finance research. We build on a long literature and make new headway. We explore the international aspect of this problem with newly-constructed data from the U.S. and 9 other advanced economies and we advance a new empirical approach which jointly disciplines estimates of the natural rate and risk premia with both financial market *and* macro information.

We first document the puzzle, for both the U.S. and other countries. For clarity, we do nothing analytically new here: we rely only on off-the-shelf models and data. The analysis revolves around three trend estimates. For the U.S., we construct an estimate of the bond risk premium following the canonical model (Adrian, Crump, and Moench, 2013) used by academic and financial professionals, and also by the Federal Reserve. We estimate inflation expectations following recent research incorporating trend inflation into models of bond yields and risk premia (Cieslak and Povala, 2015). And we employ or construct an estimate of the natural rate using the seminal model in the macro literature (Laubach and Williams, 2003). We then use directly-observed long-dated forwards to show a contradiction. In the U.S., for example, bond premia, inflation, and forwards, the implied natural rate is nearly flat over six decades, inconsistent with the rise and fall seen in macro estimates (with the implication that changes in the bond risk premium mostly explain long-yield changes). Conversely, using natural rates, inflation, and forwards, the implied bond risk premium is nearly flat, inconsistent with the rise and fall seen in finance estimates (with the implication that changes in natural rates mostly explain long-yield changes). Both models cannot be true. The puzzle is not an artifact of these particular estimates, and obtains using other well-respected estimates of U.S. bond risk premia, trend inflation, and the natural rate from multiple credible sources. The same puzzle also exists internationally in data we have newly compiled from other advanced economies.

The puzzle matters because our understanding of recent history hinges on whether one or the other story is more accurate. One narrative (macro) is of steadily declining natural real rates from the 1980s to the present, arguably culminating in a global secular stagnation trap, with active debate over a wide range of causal factors including demography and aging, productivity growth, inequality, and safe-asset demand from emerging economies, and all the attendant problems (Caballero, Farhi, and Gourinchas, 2008; Summers, 2015; Carvalho, Ferrero, and Nechio, 2016; Holston, Laubach, and Williams, 2017; Rachel and Smith, 2017; Rachel and Summers, 2019). The other narrative (finance) is of a sweeping rise and fall in risk premia, from sometime in the 1970s to the 1980s, the backwash of the Great Inflation episode, accounting for most of the trajectory of nominal rate with little or no movement in the natural rate (Kim and Wright, 2005; Wright, 2011; Adrian, Crump, and Moench, 2013; Bernanke, 2015). But when adding these up we find that something has to give.

At some level, it might be tempting to suggest that the puzzle can be brushed away with an argument that these various models from different traditions were never supposed to be coupled together in this way: finance models were not designed to be used to infer the natural rate, nor macro models to infer the bond risk premium. Yet, that is our point—and the rationale for this paper. If these models are never unified into a fully consistent approach, different strands of the literature will be destined to keep on producing contradictory results, speaking to their own niche but unable to reach common ground with the other approach. More broadly, this leaves the wider audience in macro and finance research, and in markets and the policy world, confused at to what is ultimately the right historical accounting for important long-run trends in the bond markets.

To tackle this conflict we set out a unified macro-finance model to ground the empirical work that follows. The model crystallizes the uncontroversial view—among macroeconomists, at least—that nominal bond returns must include compensation for macroeconomic risks linked to real factors and inflation (Ang and Piazzesi, 2003; Ludvigson and Ng, 2009; Cieslak and Povala, 2015).

Here, as we indicated at the start, what *we* will mean by "macro-finance" is a model that incorporates simultaneously higher-frequency insights from the yield curve in finance models and lower-frequency secular inflation and growth trends (as distinct from cyclical macro phenomena within the business cycle). Thus we have to build on the idea that term structure models should allow all nominal rates to include a slow-moving stochastic trend, as seen in early work by Campbell and Shiller (1987) and developed further in the seminal papers of Kozicki and Tinsley (2001) and Cieslak and Povala (2015), to allow yields and expected returns to bonds of different maturities derived under no-arbitrage constraints from a short-rate process linked to the two macroeconomic factors, r^* and π^*, the natural rate and inflation trends.

Next, in the empirical core of the paper, we take the model to the data. We apply the model to the postwar data (as far back as the 1950s for some countries) for 10 advanced economies, a global historical laboratory considerably larger than any previously explored in the study of these questions as far as we know. We thus develop new estimates of the natural rate covering many more countries and several more decades than prior studies: for example Holston, Laubach, and Williams (2017) cover only 4 economies from 1961 to 2015.

We find strong support for the model. Trend inflation is treated as an observable, as in prior work, but the unobservable natural rate is treated as latent and estimated from a no-arbitrage state-space model, with both macro and finance blocks, using the Kalman filter. Specifically, we make a unifying link here, by also including a macroeconomic growth driver in a Wicksellian $r^* = g + z$ state equation, in addition to a yield measurement equation, so our model utilizes information from both macro and financial market data. We therefore choose to refer to our r^* estimate as the *market-implied natural rate*.[1] Dropping either trend variable significantly worsens the model fit: the baseline R^2 statistics are relatively high, but fit worsens one or both trends are removed, especially in return forecast regressions. Indeed, the macroeconomic factors subsume much of the relevant information needed to predict returns as compared with benchmark yield-only term-structure models, leaving only detrended yields to play a role, amplifying the insight of Cieslak and Povala (2015), but now for two trends and more countries.

The main contribution of this paper is a unified model which bridges the methodological divide and exploits fully all the information used separately in previous finance and macro approaches. Summing up the model we connect to the literature and review the reasons why such an encompassing modeling approach is needed. Finance models of unobserved bond risk premia have utilized yield-based factors, Wicksellian macro models of the unobserved natural rate have utilized macroeconomic variables like growth. The two produce inconsistent results and we argue that a unified approach using both sets of information is necessary. To get there, our paper makes a number of specific points along the way, touching on questions that have emerged from distinct literatures. First, we document for many countries, over many decades, an important macro-finance puzzle which the separate paths of risk premia research and natural rate research have often skirted around. Second, to operationalize the model, we apply a joint estimation strategy; though novel, and computationally much more burdensome, this should be preferred to approaches which draw natural rate and risk premia estimates from disparate models, which can lead to inconsistency. Third, we put together a new database of zero-coupon yield curves for ten countries, a valuable data contribution in its own right for the use of future researchers. Fourth, using these data and other proxies, we present estimates from a long and wide sample of 10 advanced economies, where we find that this is not just a U.S. story and this allows us to identify diverse global trends. Fifth, our method produces improved predictions for bond yields and returns in the U.S. and international samples, including out of sample return prediction. Sixth, our natural rate estimates covary with growth and demographic variables in a manner consistent with theory and previous findings.

By the end, we are in a position to assay the natural rate puzzle, and we get a clear answer: across advanced economies, most of the long-term variation in yields in recent decades has come from shifts in the natural rate and inflation trend components, not from shifts in bond risk premia. A key takeaway is that macro and finance models do not have to go their separate ways any longer.

[1] A related and distinct model is Bauer and Rudebusch (2020), with a single stochastic trend, a nominal natural rate factor i^*. Their estimation uses yield-based factors but omits macroeconomic variables like growth in the state-space model (see their Appendix C).

2. The natural rate puzzle

The natural rate puzzle is the observation that standard finance models of bond risk premia generate a natural rate path at odds with the macro models.

In a wide class of standard stationary affine asset pricing models, the term structures (of bond yields, prices, excess returns, and forwards) are affine functions of the model's vector of risk factors F which will be made precise in the next section. As we will formally demonstrate below, in a typical such model we can express the very-long maturity forward rate, in the asymptotic limit, as

$$\text{limiting forward rate} = \text{natural rate trend} + \text{inflation trend} + \text{limiting risk premium}. \quad (1)$$

This expression is intuitive. Investors in long maturity forwards must be compensated by the sum of the natural rate and inflation, plus a term that is by definition the long bond risk premium. The seminal work of Kozicki and Tinsley (2001) captures this in a term structure model with a "shifting endpoint" and they found improved fit when the endpoint was inferred from long-dated forwards.

If extant models were consistent, we could empirically validate Equation 1 by taking proxies for each term and checking to see if they add up appropriately. We do this as follows. We naïvely take the limiting risk premium (denoted Γ) from benchmark models in the finance literature, we take the natural rate trend (denoted r^*) and the inflation trend (denoted π^*) from benchmark macro models, and take a proxy limiting forward rate (denoted f) from long-dated market data. Having constructed these four terms for multiple countries, we can show that the above equation fails to hold. This is what we term the natural rate puzzle.

This section sets out to document this fact across the advanced economies and the rest of the paper explores a hybrid macro-finance model which may offer a way out. As might be anticipated, Equation 1 offers only two escape routes. Given that the forward rate is an observed trending variable, and that the observed inflation trend π^* is not subject to large estimation error, or can be treated as quasi-observable, then either the trend in the natural rate r^* is mismeasured, or the trend in the risk premium Γ is mismeasured, or both.

2.1. U.S. evidence

To see the puzzle, we take Equation 1 directly to the data. In Figure 1, Panel (a), the U.S. time-series estimates for each of the four terms are shown. We simply take these estimates from canonical models in the finance and macro literatures. The bond risk premium term Γ (two-sided) is from the baseline five-factor model of Adrian, Crump, and Moench (2013) [henceforth abbreviated ACM]; the inflation expectations term π^* is the Cieslak and Povala (2015) measure $\pi_t^* = (1-\nu)\sum_{i=0}^{t-1} \nu^i \pi_{t-i}$, where π_t is year-on-year CPI inflation in month t. and the (two-sided) natural rate term r^* as in Laubach and Williams (2003) [LW]. Finally, we proxy f with the long-dated 10-year, 10-year forward rate taken from Bloomberg, with $n = m = 120$ months here.

Figure 1: *The natural rate puzzle in U.S. data*

This figure displays market data (f) and existing trend data (other variables) based on other studies in Panel (a), and then displays the puzzle in the form of the difference between existing trend data and implied data in Panels (b) and (c). The presentation is based on Equation 1, which we can rewrite in simplified form, omitting subscripts and expectations, and taking them as understood, with the notation $f = r^* + \pi + \Gamma$. The puzzle is that existing benchmark estimates violate this equation.

In Panel (a), the four terms are shown: the bond risk premium Γ from Adrian, Crump, and Moench (2013); inflation expectations π from Cieslak and Povala (2015); and the real natural rate r^* from Laubach and Williams (2003). We also show the 10-year, 10-year forward rate (f) from from Bloomberg. The sample period is June 1961–July 2022. In Panel (b), we compare the real natural rate r^* (two-sided) from Laubach and Williams (2003) to that implied by $r^* = f - \pi^* - \Gamma$. There is a large difference between these two series. In Panel (c), we compare the bond risk premium Γ (two-sided) from Adrian, Crump, and Moench (2013) to that implied by $\Gamma = f - r^* - \pi^*$. There is the same large difference between these two series.

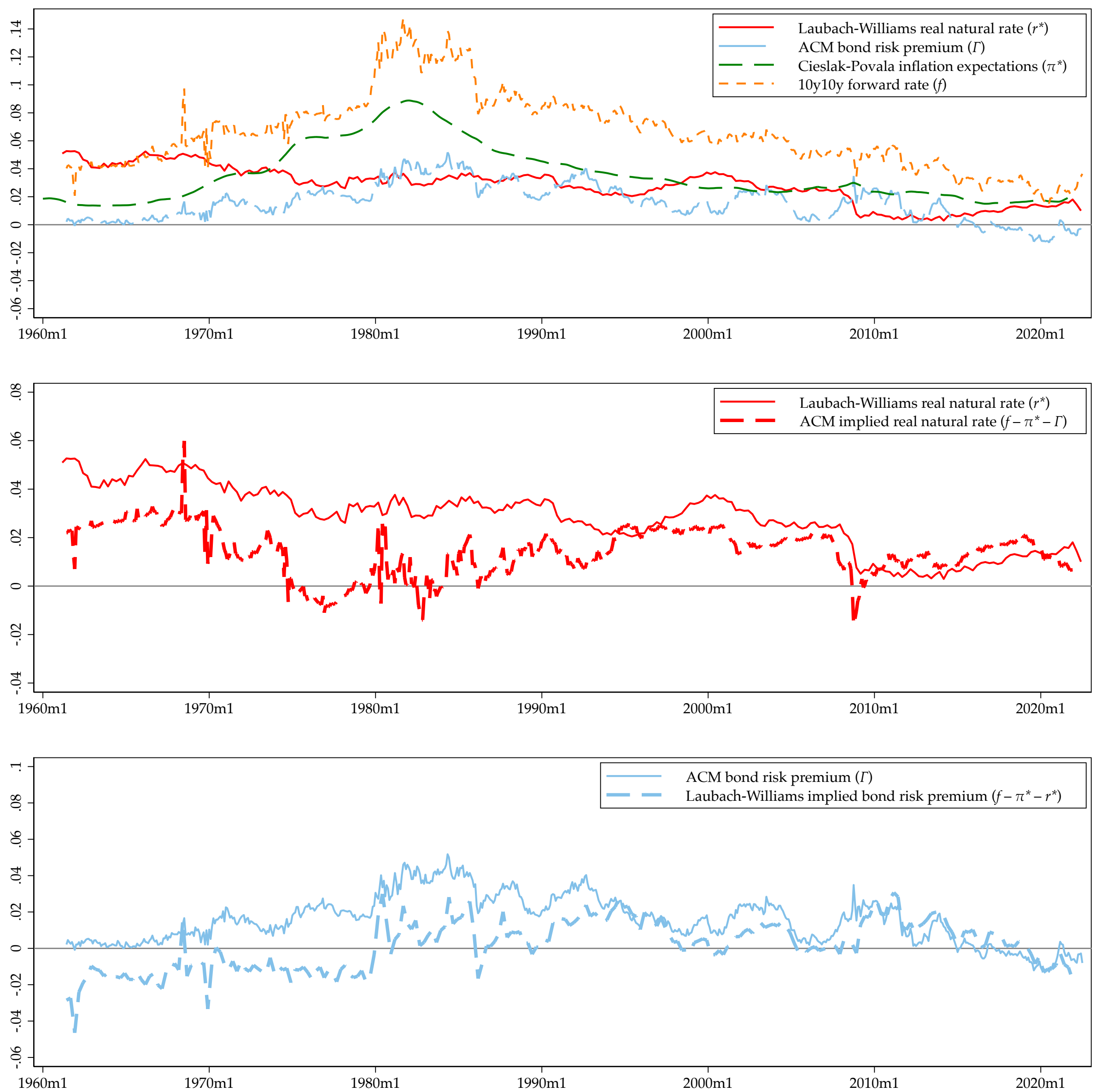

The first version of the consistency test rearranges Equation 1 to obtain a formula for the real natural rate $r^* = f - \pi^* - \Gamma$, and Panel (b) plots both sides of this expression using the above data sources: the left-hand side is taken from an LW model and the right-hand side is the implied value using an ACM model. The equality is violated, and the disparity is often quite large. The ACM-implied r^* does not match the LW r^*. The ACM series starts around +2% in the 1960, displays a sharp decline to a level below −2% during the Great Inflation period of the 1970s, returns to +2% in the 1990s, drops to near zero after the financial crisis, and then shows a consistent increase after 2013 to a level close to 2% in 2019. In contrast, the familiar LW estimate of r^* has fallen gradually from a +4% level in the 1960s and 1970s, with the sharpest decline occurring after the mid-2000s, and since 2010 it has sat in the 0.5%–1.0% range, and never turned negative. The difference between the two series, before the last decade, is often large, between 100 and 600 basis points (bps), with the LW r^* much higher than the ACM r^*, on average. Around 2012 the two series intersected and then the difference inverted to about −100 bps in the other direction.

A second, equivalent, version of the test is shown in Panel (c). We rearrange again to obtain a formula for the bond risk premium $\Gamma = f - r^* - \pi^*$, and Panel (b) plots both sides of this expression using the aforementioned data sources. Now the left-hand side is from an ACM model and the right-hand side is the implied value in an LW model. This equality is, of course, also violated, and the same large disparity is seen. The ACM bond risk premium starts near zero in the 1960s, rises sharply in the Great Inflation period of the 1970s to about 6%, then gradually falls back, reaching zero again in the mid-2010s. The LW bond risk premium behaves very differently, and is almost flat by comparison. It actually starts at a negative level in the 1960s, rises much later, but only to a modest 2% by the early 1980s, then declines by a small amount up to the mid 2000s. After that the two series cross, with LW signaling a small positive bond risk premium, but ACM turning negative.

The puzzle is vividly apparent in these charts. Persistent inconsistencies of several hundred basis points are quantitatively just too large to ignore. Both approaches cannot be simultaneously right. A substantial contradiction thus emerges from the heart of benchmark macro and finance models once they are studied in unison. The rest of this paper is devoted to building theory and empirics to help resolve the puzzle.

2.2. Alternative trend measures

As a robustness check, Figure 2 examines whether the existence of the puzzle for the U.S. is sensitive to the source data used. For a variety of widely used and respected sources we compute the discrepancy in Equation 1 as $\textit{discrepancy} = r^* - f + \pi^* + \Gamma$, and plot the series over time.

The same forward rate data f from Bloomberg are used in all cases. The sources of the other three series rotate through all possible combinations, with the sources are abbreviated as follows:

- Natural rate estimates r^*: Laubach and Williams (2003) [LW]; Holston, Laubach, and Williams (2017) [HLW]; Del Negro, Giannone, Giannoni, and Tambalotti (2017) [DGGT]; and Lubik and Matthes (2015) [LM].

Figure 2: *The natural rate puzzle in U.S. data using alternative trend measures*

This chart displays the discrepancy in Equation 1 for the United States. The presentation is based on Equation 1 and the series computed is *discrepancy* = $r^* - f + \pi^* + \Gamma$. See text.

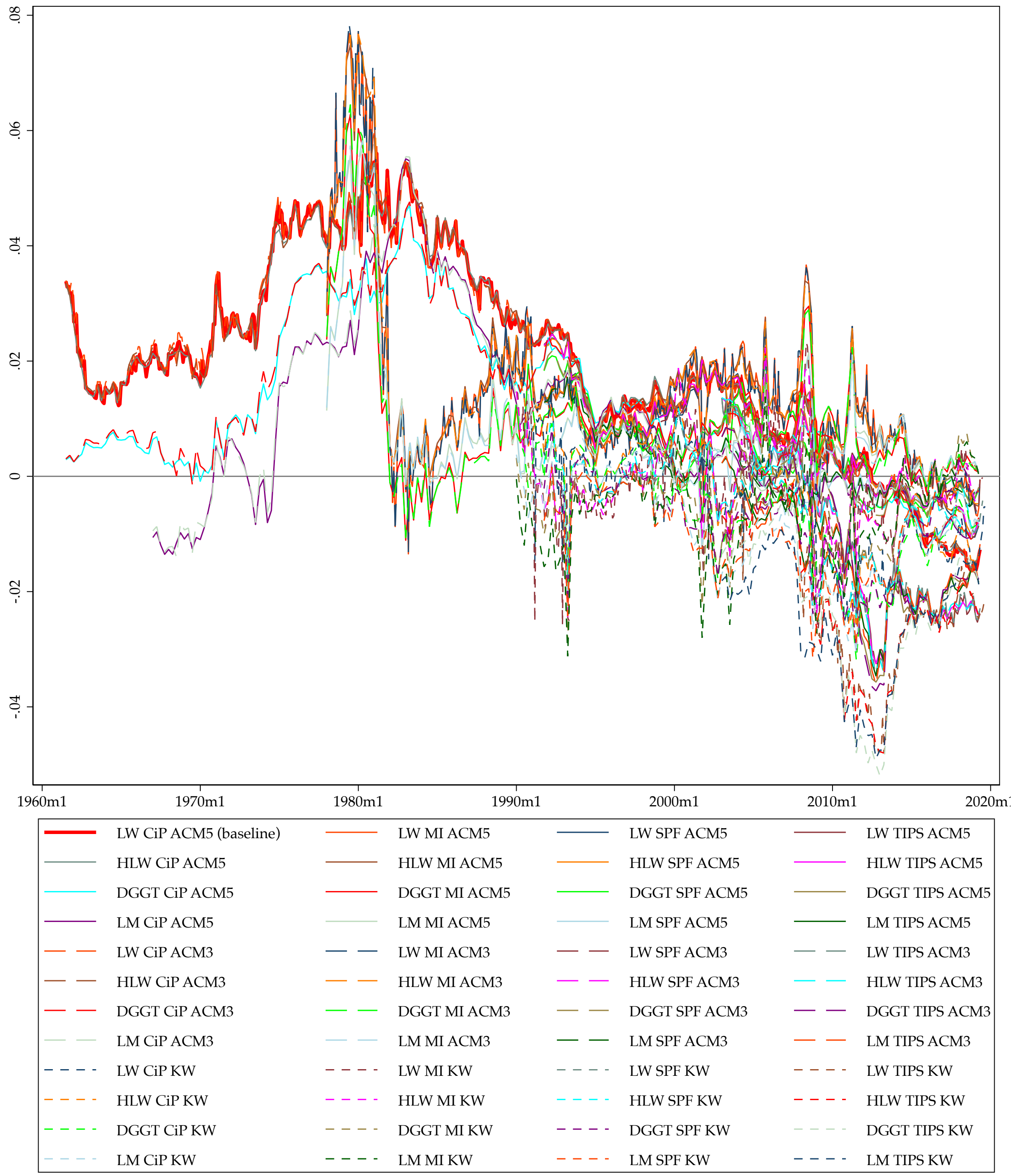

- Inflation estimates π^*: Cieslak and Povala (2015) [CiP]; the University of Michigan Inflation Expectations from FRED [MI]; the Survey of Professional Forecasters from the Federal Reserve Bank of Philadelphia [SPF]; and the TIPS 10-Year Breakeven Inflation Rate from FRED [TIPS].
- Bond risk premium estimates Γ: Adrian, Crump, and Moench (2013), 5-factor model [ACM5]; the same authors' 3-factor model [ACM3]; and Kim and Wright (2005), 3-factor model [KW].

Note that because quite a few of these series (e.g., TIPS, KW) are only available for a shorter span of recent years, full-sample comparisons across all trend estimates are not always possible.

The figure reveals that the natural rate puzzle is a quite robust phenomenon in recent U.S. data. A discrepancy arises in all cases. It is often more than 100 bps, and at certain times it exceeds 500 bps. It is present in a wide variety of trend estimates currently used in the macro-finance literatures. The figure shows that, as in the baseline variant above, the extent of the puzzle varies from year to year, and over decades. Most series combinations make errors in one direction, but a few go the other way. The discrepancies are large in the 1970s, and often surge to their highest levels around 1980. The discrepancies are smaller by the late 1990s and early 2000s, but they open up again for some series, in the opposite direction to the vicinity of –400 bps, after the global financial crisis.

2.3. International evidence

We also sought evidence for or against the natural rate puzzle in 5 other advanced economies: Japan, Germany, the U.K., Canada, and Australia. Figure 3 presents these findings. For the real natural rate we use an established r^* from an LW- or HLW-type model, the risk premium from an ACM-type estimation, inflation expectations from a CiP-type estimation, and the forward rate. However, established natural rate estimates of an LW- or HLW-type are only available for 6 out of our 10 sample countries, and so we cannot perform this exercise for France, Spain, Sweden, and Switzerland.

For the LW-type natural rate estimates we use the LW estimate itself for the U.S. as above; the Holston, Laubach, and Williams (2017) (two-sided estimates) for the Germany, U.K., and Canada; the Okazaki and Sudo (2018) (two-sided estimates) for Japan, and the McCririck and Rees (2017) (two-sided estimates) for Australia. We then replicate the ACM and CiP methodologies for these 6 countries and construct forward rates from zero-coupon bonds, as described later in this paper, and finally compute the discrepancy for all the countries to complete the analysis, with $\textit{discrepancy} = r^* - f + \pi^* + \Gamma$, as above.

The discrepancy can be visualized over time in Figure 3, which presents the time-series data for each natural rate estimate. Here again, discrepancies of several hundred basis points are not uncommon. In short, the natural rate puzzle is not simply a U.S. puzzle. It applies to many advanced economies, suggesting a deeper and more general pattern of conflict between widely-used standard estimates of the natural rate and bond risk premia.

Figure 3: *The natural rate puzzle in international data*

This chart displays the discrepancy in Equation 1 for the set of 6 countries. The presentation is based on Equation 1 and the series computed is *discrepancy* = $r^* - f + \pi^* + \Gamma$. See text.

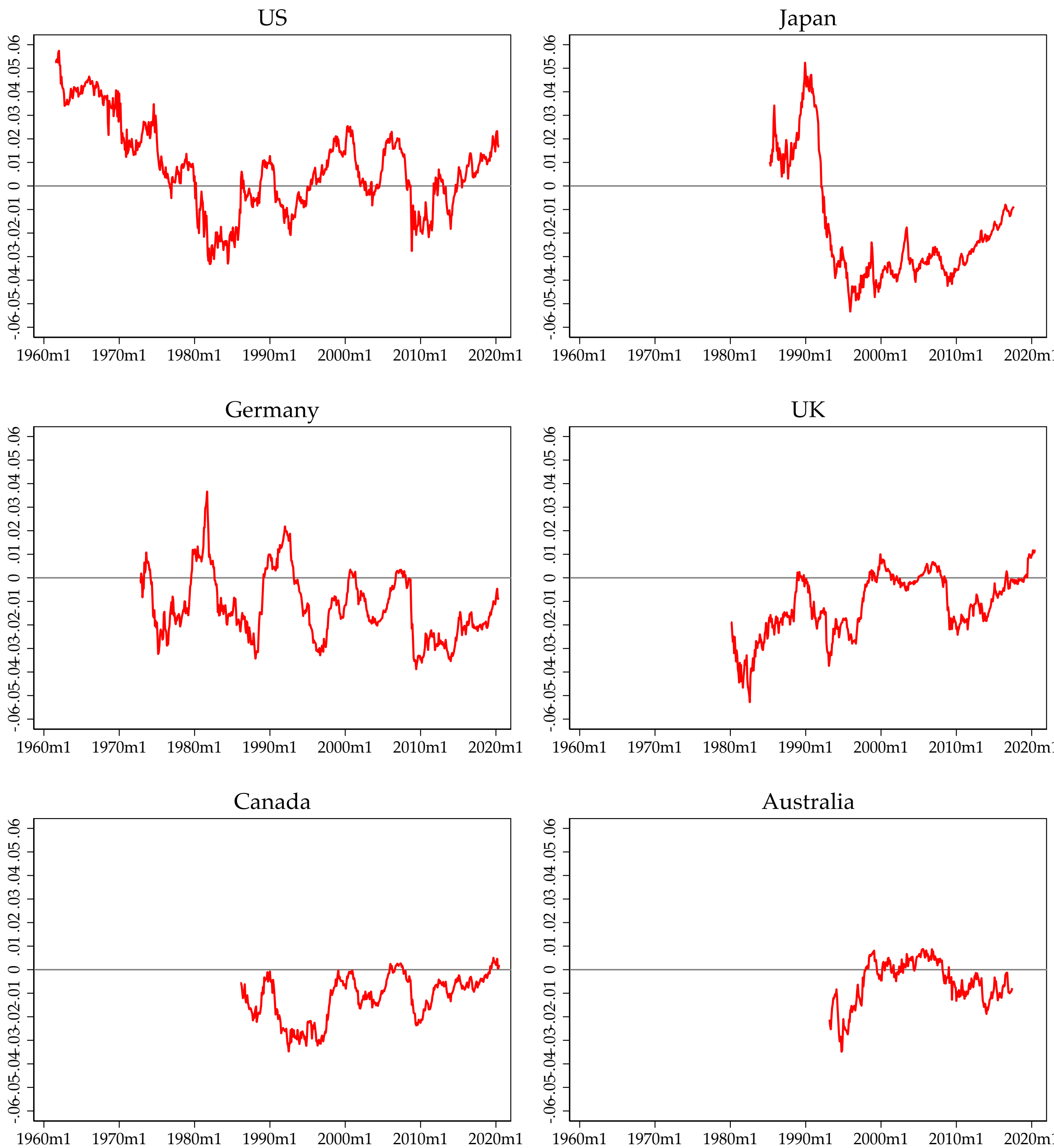

3. Term-structure models with two macro factors

A large literature over 20 years has built a foundation of affine term-structure models with a role for macroeconomic trends in inflation and the natural rate. Building on that we ask: first, can theory frame the natural rate puzzle seen above? Second, can joint estimation of the natural rate and the term-structure model deliver new insights and better forecasts? Third, can the approach work not just in U.S. data but also in other advanced economies? We will answer yes to these questions based on the approach described in this section.

Stationary term-structure model We use a standard setup as in the seminal paper of Cieslak and Povala (2015) which features two trends for inflation and the real rate, building on the earlier insights of Kozicki and Tinsley (2001). At time t, we denote the nominal yield on an n-period Treasury bond by $y_t^{(n)}$, the current trend inflation by π_t, and the current trend real natural rate by r_t. Nominal yields across all maturities are driven by the two trends and other factors contained in a price-of-risk factor x_t vector, so the full set of factors is $F_t = (\pi_t, r_t, x_t)'$. Building on, Cieslak and Povala (2015) as a baseline we will set x_t equal to the average yield across the curve, or, equivalently (as we see below) its residual component after projection onto the two macro trends (π_t, r_t).

The core of the model is the specification of the short-rate process and the stochastic discount factor, from which all other pricing relationships follow. The short-rate process is assumed to depend on the factors, which in turn follow independent AR(1) processes, with

$$y_t^{(1)} = \delta_0 + \delta_\pi \pi_t + \delta_r r_t \,, \tag{2}$$

$$r_t = \mu_r + \phi_r r_{t-1} + \sigma_r \epsilon_t^r \,, \tag{3}$$

$$\pi_t = \mu_\pi + \phi_\pi \pi_{t-1} + \sigma_\pi \epsilon_t^\pi \,, \tag{4}$$

where $\delta_\pi > 0, \delta_r > 0$, with $\delta_x = 0$, as shown, and $\epsilon_t^\pi, \epsilon_t^r$ are standard normal, i.i.d.

At Equation 2, a natural benchmark noted by Cieslak and Povala (2015) is $\delta_0 = 0, \delta_\pi = \delta_r = 1$, i.e., the Fisher constraints. At Equation 3 and Equation 4, with persistent inflation we expect $\phi_\pi < 1$ but close to unity. The natural rate also tends to be persistent, with $\phi_r < 1$ and close to unity. In very long run historical data (100+ years) both series are seen to be stationary. Cieslak and Povala (2015) estimate annual $\hat{\phi}_\pi = 0.975$, $\hat{\phi}_r = 0.75$ for their U.S. sample.

The *endpoints* for the trends are the long-run limits (Kozicki and Tinsley, 2001). Allowing for possibly time-varying parameters the unconditional means of the endpoints are $r_\infty^{(t)} = \mu_r^{(t)}/(1-\phi_r^{(t)})$ and $\pi_\infty^{(t)} = \mu_\pi^{(t)}/(1-\phi_\pi^{(t)})$. These values prevail in the long run when all shocks have died out.

Finally, the price-of-risk factor follows an AR(1) process with i.i.d. normal shocks,

$$x_t = \mu_x + \phi_x x_{t-1} + \sigma_x \epsilon_t^x \,. \tag{5}$$

Cieslak and Povala (2015) estimate $\hat{\phi}_x = 0.392$ for the U.S. when detrending with the inflation trend.

The model economy is then compactly described by the equations

$$F_t = \mu + \Phi F_{t-1} + \Sigma \epsilon_t \,, \tag{6}$$

$$y_t^{(1)} = \delta_0 + \delta_1' F_t \,, \tag{7}$$

with Φ and Σ diagonal, $\delta_1 = (\delta_\pi, \delta_r, 0)'$, and $\epsilon_t = (\epsilon_t^\pi, \epsilon_t^r, \epsilon_t^x)'$.

As is common, the simplest single-yield-factor formulation would define $x_t = \bar{y}_t$, so the price-of-risk factor is the average level of yields, $\bar{y}_t = \frac{1}{N}\sum_1^N y_t^{(n)}$.[2] Clearly then, in light of our earlier discussion, this is (see Duffee, 2011) a "yields-plus" model and not a "yields-only" model. That is, we are interested in whether the two macro trends r_t and π_t add useful information over and above a model using just a set of yield-based factors.

Our choice of $F_t = (\pi_t, r_t, x_t)^\top$ follows Cieslak and Povala (2015) and assumes that $\epsilon_t^\pi, \epsilon_t^r$ are uncorrelated. Thus, the natural rate factor r_t is intended to capture variations in the benchmark real rate due to factors other than shifts in trend inflation. Equation 2 specifies in a stylized way how monetary policy, through its control of the short end of the curve, may react to both changes in price dynamics and real-economy-driven natural rate forces. A large stream of literature has related these forces to demographic factors, global supply and demand equilibrium in the safe-assets market, changes in international capital flows, income and wealth inequality, among others.

Imposing standard restrictions on the model SDF Using a standard no-arbitrage affine term-structure model as in Cieslak and Povala (2015), the log nominal stochastic discount factor is exponentially affine in the risk factors,

$$m_{t+1} = -y_t^{(1)} - \frac{1}{2}\Lambda_t'\Lambda_t - \Lambda_t'\epsilon_{t+1} \,, \tag{8}$$

where Λ_t is the compensation for risk of shock ϵ_{t+1}, with $\Lambda_t = \Sigma^{-1}(\lambda_0 + \Lambda_1 F_t)$.

We need more structure to make progress. Suppose x_t is taken to be a single yield-based factor, and the loadings in Λ_t are assumed to take the form

$$\lambda_0 = \begin{pmatrix} \lambda_{0\pi} \\ \lambda_{0r} \\ 0 \end{pmatrix}, \qquad \Lambda_1 = \begin{pmatrix} 0 & 0 & \lambda_{\pi x} \\ 0 & 0 & \lambda_{rx} \\ 0 & 0 & 0 \end{pmatrix}. \tag{9}$$

As Cieslak and Povala (2015) note, this setup fits with the empirical finding of Cochrane and Piazzesi (2005) that bond risk premiums move on a single mean-revering factor that is largely unexplained by the level, slope, and curvature movements. In this spirit, as is seen in a wide range

[2]This baseline setup is motivated by the Cochrane and Piazzesi (2005) finding that a single-factor can explain bond pricing quite well, but x could be expanded to a vector as in three-factor yield models (Nelson and Siegel, 1987; Litterman and Scheinkman, 1991; Joslin, Singleton, and Zhu, 2011) or even five-factor yield models (Adrian, Crump, and Moench, 2015).

of established term structure models, the price of risk is assumed to follow a univariate process that is independent of other state variables. Cieslak and Povala (2015) estimate $\hat{\lambda}_{\pi x} = -0.47$ and $\hat{\lambda}_{rx} = 0.16$ for their U.S. sample.

Solving the model The model can then be solved (e.g., Duffee, 2013) as a set of affine equations for log bond prices, yields, forwards, and excess returns, in terms of the factors:

$$p_t^{(n)} = \mathcal{A}_n + \mathcal{B}_n' F_t \,, \tag{10}$$

$$y_t^{(n)} = A_n + B_n' F_t \,, \tag{11}$$

$$f_t^{(n,m)} = (\mathcal{A}_n - \mathcal{A}_{n+m}) + (\mathcal{B}_n - \mathcal{B}_{n+m})' F_t \,, \tag{12}$$

$$rx_{t+1}^{(n)} = \mathfrak{B}_n' F_t + v_t^n \,, \tag{13}$$

where $A_n = -\frac{1}{n}\mathcal{A}_n$, $B_n = -\frac{1}{n}\mathcal{B}_n$, $v_t^n = \mathcal{B}_{n-1}' \Sigma \epsilon_{t+1}$.

Solutions are derived from Riccati equations, where the recursions are

$$\mathcal{A}_{n+1} = -\delta_0 + \mathcal{A}_n + \mathcal{B}_n' \mu^q + \frac{1}{2} \mathcal{B}_n' \Sigma \Sigma' \mathcal{B}_n \,, \tag{14}$$

$$\mathcal{B}_{n+1} = -\delta_1 + (\Phi^q)' \mathcal{B}_n \,, \tag{15}$$

with $\mathcal{A}_0 = 0$, $\mathcal{B}_0 = 0$, and risk-neutral dynamics governed by $\mu^q = \mu - \lambda_0$ and $\Phi^q = \Phi - \lambda_1$.[3]

Concretely, in the baseline model used here, factor loadings of bond prices can be derived as

$$\mathcal{B}_n^{\pi} = -\delta_{\pi} \frac{1 - \phi_{\pi}^n}{1 - \phi_{\pi}} \,, \tag{16}$$

$$\mathcal{B}_n^{r} = -\delta_{r} \frac{1 - \phi_{r}^n}{1 - \phi_{r}} \,, \tag{17}$$

$$\mathcal{B}_n^{x} = -\mathcal{B}_{n-1}^{\pi} \lambda_{\pi x} - \mathcal{B}_{n-1}^{r} \lambda_{rx} + \mathcal{B}_{n-1}^{x} \phi_x \,, \tag{18}$$

and the factor loadings of excess returns attach only to the price-of-risk factor, with

$$\mathfrak{B}_n = \mathcal{B}_{n-1}' (\lambda_0 + \Lambda_1 \mathbf{1}_3) x_t - \frac{1}{2} \mathcal{B}_{n-1}' \Sigma \Sigma' \mathcal{B}_{n-1} \,. \tag{19}$$

Equivalent formulation using detrended yields As above, we might set $x_t = \bar{y}_t$, so the price-of-risk factor is the average level of yields. But to better describe the role of the trends we use the key innovation in Cieslak and Povala (2015), and reformulate the model using yields which have been *detrended* to orthogonalize them relative to the trends. We apply this idea to *both* trends, and define the detrended yield by $c_t^{(n)} = y_t^{(n)} - \hat{A}_n - \hat{B}_n^r r_t - \hat{B}_n^{\pi} \pi_t$, which is the residual from the regression defined by Equation 11 with the yield factor x suppressed. Now let the average of this detrended yield be $\bar{c}_t = \frac{1}{N} \sum_1^N c_t^{(n)}$.

[3] The closed form solution for $\mathcal{B}_n$ is $\mathcal{B}_n = -\left[\sum_{j=0}^{n-1} (\Phi^q)^j\right]' \delta_1$.

The model can then be expressed in our preferred form in terms of $x_t = \bar{c}_t$ and the full set of factors consists of the two trends and the detrended average yield, $F_t = (\pi_t, r_t, \bar{c}_t)'$. Due to detrending, in this setup the unconditional mean of F_t is now $\mu = E(F_t) = (\pi_\infty^{(t)}, r_\infty^{(t)}, 0)$. To be clear, this reformulation leaves the model unchanged, but this attribution exercise parses out those shifts in yield factors that are ultimately driven by the macro trends.

Statistical identification of the natural rate of interest A crucial step in affine models with trends is to obtain the right trends. Ever since Kozicki and Tinsley (2001) and Cieslak and Povala (2015), the literature takes inflation as observable $\pi_t = \pi_t^*$, e.g., from surveys or a learning model. However, the natural rate is unobserved or latent. One of our contributions is to focus on the joint problem of estimating both the affine model and the natural rate in a consistent framework.

We propose a way to bridge the statistical objects specified in Equation 2 through Equation 4 to the economic object of interest, the natural rate, consistent with the Wicksellian notion of r^*. To do this we link the natural rate to variations in trend growth g_t plus an additional component denominated the "headwinds" factor z_t, as in canonical state-space models of the natural rate. Thus, we aim to straddle the yields-plus approach of finance models and the Wicksellian estimation of macro models in the tradition of Laubach and Williams (2003), and this entails adding the equation:

$$r_t = r_t^* = z_t + g_t \,. \tag{20}$$

The headwinds factor is intended to capture all variations in the natural rate due to structural, slow-moving factors such as demographics, structural shifts in international capital flows, global income inequality, among others. The coefficient on g_t is in general $c \neq 1$, and is equal to the inverse EIS. It is set here to a reference value of one for simplicity, given the considerable uncertainty over the appropriate value of EIS in the macro and finance literatures. This is consistent with the four estimates of c in Table 2 of Laubach and Williams (2003) which fall in the range 0.970 to 1.062.

We also assume that the headwinds factor follows an AR(1) process, so that

$$z_{t+1} = \rho_z z_t + e_{t+1}^z \,, \qquad e_{t+1}^z \sim N\left(0, \sigma_z^2\right) \,. \tag{21}$$

Without any constraints, the headwinds factors would absorb all the high frequency variation in rates. We argue that the frequency and persistence of the headwinds factor should be more like the process followed by trend growth than, say, yields. In order to discipline this process, and make its frequency compatible with the fundamental growth trends observed, we impose suitable priors on ρ_z and σ_z, as discussed below and in Appendix A. These priors force the headwinds process to follow a lower frequency than financial data (yields, etc.), without forcing a link from the natural rate to particular economic data, other than the Wicksellian link to growth g.

Trend output growth g_t is assumed to be a stationary process and observable. We take it as an exogenous process that we can estimate separately by typical filtering procedures. To avoid forward-looking bias, we estimate the as-of-date (one-sided) Hodrick-Prescott filter on country real GDP growth (to be conservative, when calculating the growth rate at t, we use information available at time $t-1$, namely growth rates up to $t-2$).

The above steps harmonize our state-space model with the macro approach to interest rate trends epitomized by Laubach and Williams (2003). Full details of the state-space model follow in the next section and, in detail, in the Appendix. For now we cover some further ground to explain how this approach connects to the natural rate puzzle presented earlier, and how it contributes to the literature.

Corollary 1: Long-dated forwards, macro trend endpoints, and the bond risk premium
Using the baseline model we can provide justification for the decomposition at Equation 1 to introduce the natural rate puzzle.

For a 1-period forward at horizon n, $f_t^{(n,1)} = (\mathcal{A}_n - \mathcal{A}_{n+1}) + (\mathcal{B}_n - \mathcal{B}_{n+1})' F_t$ and from the recursions (e.g., Duffee, 2013) we obtain

$$f_t^{(n,1)} = \underbrace{-\frac{1}{2}\mathcal{B}_{n-1}'\Sigma\Sigma'\mathcal{B}_{n-1}}_{\text{negative convexity term}} + \underbrace{\delta_0 - \mathcal{B}_n'\mu^q + \delta_1'(\Phi^q)^n F_t}_{\text{expected short rate under } q} . \tag{22}$$

Let the benchmark Fisher constraints hold, $\delta_0 = 0, \delta_\pi = \delta_r = 1$, substitute for μ_i, and we have

$$\lim_{n\to\infty} f_t^{(n,1)} = \underbrace{r_\infty^{(t)}}_{\substack{\text{endpoint for}\\ \text{natural rate}}} + \underbrace{\pi_\infty^{(t)}}_{\substack{\text{endpoint for}\\ \text{inflation}}} + \underbrace{\mathcal{B}_\infty^\pi \lambda_{0\pi} + \mathcal{B}_\infty^r \lambda_{0r} - \frac{1}{2}\mathcal{B}_\infty'\Sigma\Sigma'\mathcal{B}_\infty}_{\text{bond risk premium as } n\to\infty} . \tag{23}$$

Thus the limiting forward rate equals the sum of the natural rate and inflation endpoints and the limiting bond risk premium.[4] Intuitively, at shorter maturities the difference between the forward and the sum of the two endpoint will also be affected by transitory variation in short-rate expectations (i.e., due to the term $\delta_1'(\Phi^q)^n F_t$); in the long-horizon limit we get the non-transitory limiting bond risk premium, and short-term expectation deviations fade away, as Equation 23 shows.

Thus, in the limit at large maturities, or in a large sample limit where the mean of x_t is zero, we obtain an expression which justifies our earlier exercise using Equation 1,

$$\text{forward rate} = \text{natural rate trend} + \text{inflation trend} + \text{bond risk premium}\,,$$

where we associate the endpoints with the natural rate trend and inflation trend. We now see how the limit result using forwards frames the puzzle in a clean way. This approach can be complemented by an examination of the direct implications of different specifications of affine term structure models on observables such as yields, forward rates, and excess bond returns.

[4] As $n\to\infty$, $\mathcal{B}_n^\pi \to -\pi_\infty^{(t)}/\mu_\pi$, $\mathcal{B}_n^r \to -r_\infty^{(t)}/\mu_r$, and $(1-\phi_x)\mathcal{B}_n^x \to \lambda_{\pi x}\pi_\infty^{(t)}/\mu_\pi + \lambda_{rx} r_\infty^{(t)}/\mu_r$, with $\mu_c = 0$.

Corollary 2: Expected returns and the cyclical factor We can also solve (e.g., Duffee, 2013) for the factor loadings of excess returns,

$$rx_{t+1}^{(n)} = \mathcal{B}_{n-1}'(\lambda_0 + \Lambda_1 F_t) - \frac{1}{2}\mathcal{B}_{n-1}'\Sigma\Sigma'\mathcal{B}_{n-1} + \mathcal{B}_{n-1}'\Sigma\epsilon_{t+1}\,. \tag{24}$$

Setting $x_t = \bar{c}_t$, the expected return for the average bond across all maturities is

$$E_t(\overline{rx}_{t+1}) \;=\; \underbrace{(\overline{\mathcal{B}}^{\pi}, \overline{\mathcal{B}}^{r})'(\lambda_{0\pi} + \Lambda_{\pi x}\bar{c}_t, \lambda_{0r} + \Lambda_{rx}\bar{c}_t) \;-\; \text{convexity terms}}_{\text{bond risk premium for average bond}}\,. \tag{25}$$

As n grows large the average risk premia in Equation 23 and Equation 25 are the same. Note that, with detrending, i.e., having conditioned on trends, only the cyclical factor $x_t = \bar{c}_t$ predicts bond excess returns, and not the trends themselves r_t and π_t. Of course, this does *not* mean than shifts in r_t and π_t play no role: they will of course change the cyclical deviation $x_t = \bar{c}_t$ via detrending.

The nonstationary case Recent contemporaneous work by Bauer and Rudebusch (2017, 2020) studies the trends in the U.S. case and allows the trends to be nonstationary. Bauer and Rudebusch (2017) extend Cieslak and Povala (2015), and allow the factor process to include unit roots in r and π, as well as short run AR(1) disturbance terms, with 5 state variables instead of 3. The two corollaries noted above are preserved exactly, and the endpoints are the current values of the r and π, the expected values as $t \to \infty$. The loadings on the permanent components of r and π are unity at all horizons, so the Fisher constraints hold mechanically. In Bauer and Rudebusch (2020, see Appendix C) a different theoretical framework is used as a backdrop. In the real-world measure there is a unit root in a single nominal natural rate trend (i^*) and three stationary cyclical yield factors. The model could be extended to two trends and/or fewer yield factors. The model is restricted to be stationary under the risk-neutral measure, and thus threads a new path between widely-used stationary models (Cieslak and Povala, 2015) and models with unit roots under both measures (Kozicki and Tinsley, 2001).[5] The corollaries stated in the previous section no longer hold exactly, but empirically there is very close alignment.[6] In this sense, the key empirical lessons still remain intact for this case when compared with the baseline stationary setting.

Summary: Bridging three interest rate traditions The modeling of interest rates is one of the oldest questions in economics. We can now clarify how this paper falls between two distinct approaches, the purely macro and purely finance approaches, with some important precursors.

[5]The model is unspanned, and the yield curve does not contain all relevant information for predicting future interest rates. The Fisher constraints hold on the short rate, but forwards and excess returns now load on the trend in a different way. Unit loadings down the yield and forward curves are not implied here, a prediciton that might better fit the data.

[6]This is demonstrated by Bauer and Rudebusch (2020, see Appendix C): for forwards, at *practically relevant* horizons in the data (e.g., up to 15 years), the loadings on the trends are very close to one (and simulated confidence intervals are wide); and for excess returns, loadings on non-cyclical factors are close to zero, and second order.

The pure *finance approach* uses information purely from financial markets, with no macroeconomic variables. Here, the yields-only model is the starting point of all affine term structure models (Duffie and Kan, 1996; Piazzesi, 2010). The simplest model uses a single factor, the average level of yields, or a tent-shape weighted average (Cochrane and Piazzesi, 2005). More refined models may include 3 or 5 yield factors, using level-slope-curvature or principal components (Litterman and Scheinkman, 1991; Kim and Wright, 2005; Adrian, Crump, and Moench, 2015). In the pure form of this approach no macroeconomic information is used.

The pure *macro approach* focuses on a latent trend in the natural rate. These state-space models are grounded in the Wicksellian equation $r^* = g + z$, where the latent trend is disciplined by information on the real growth rate of the economy, and no financial market information is used (Holston, Laubach, and Williams, 2017; Laubach and Williams, 2003). To extend from this estimation approach to a latent nominal natural rate trend, one might then call upon the Fisher conditions, to solve for a nominal yield level $y = \pi^* + r^*$. Here survey expectations or a backward-looking learning model can be used to treat π^* as an observable, not latent variable.

A third way in the literature is a hybrid *macro-finance* approach and into which our paper fits. This large tradition has many different ingredients, so we must situate our paper properly, and our approach using inflation and natural rate trends overlaps with some but by no means all antecedents in this literature. Since at least Campbell and Shiller (1987), the literature has considered stochastic trends. One strand includes Ang and Piazzesi (2003) and Ludvigson and Ng (2009) who brought macro factors and latent factors into an affine term structure model, but without specifically the Wicksellian equation $r^* = g + z$. Kozicki and Tinsley (2001) argued that a "shifting endpoint" inferred from long-dated forwards delivered a marked improvement when added to a term structure model, while Cieslak and Povala (2015) located the inflation trend as one such factor. Both left a Wicksellian estimation equation of the real rate trend to one side. So too did Bauer and Rudebusch (2020), who used either external observed trend estimates of the natural rate from the macro literature, or an internally estimated natural rate not governed by the Wicksellian equation.[7]

Now our point of departure comes into focus: without *joint* estimation of a macro Wicksellian equation $r^* = g + z$ *and* the affine model of yields, other approaches must take sides. On the one hand, a yields-only finance model has an implied endpoint, but ignores information in the Wicksellian condition $r^* = g + z$ to guide its estimate. On the other hand, macro models (e.g., Holston, Laubach, and Williams, 2017; Laubach and Williams, 2003) use the Wicksellian equation but information in yields play no role. The two types of natural rate estimates must, in general, differ; symmetrically, the same disparity will manifest in implied bond risk premia too, given observable forwards and the inflation trend, as we saw earlier. As we see it, this is the heart of the natural rate puzzle, and it is this tension that we set out to resolve.

[7]Their estimated-shifting-endpoint model has no Wicksellian equation, one trend $\tau = i^* = r^* + \pi^*$, with trend estimation disciplined with priors similar to Del Negro, Giannone, Giannoni, and Tambalotti (2017).

4. Reduced-form model estimation and model evaluation

Taking the above structural model as given, we operationalize it via the following Bayesian reduced-form estimation method, as in common. From now on, we restore the star notation, and denote by r_t^* the trend natural rate, and by π_t^* trend inflation. We aim to extract the latent r_t^* from average bond yields by using state-space estimation with an affine measurement equation of the form:

$$\bar{y}_t = a_y + b_\pi \pi_t^* + b_r r_t^* + \epsilon_t^{cyc}, \tag{26}$$

where π_t^* is trend inflation, a variable which is treated as an observable, and for each country is set equal to the Cieslak and Povala (2015) measure. This equation can be seen as deriving from the structural Equation 11 with $y_t^{(n)} = A_n + B_n' F_t$ averaged over all maturities, 1 to 180 months. (One could entertain model variants with more points across the curve are more difficult to estimate without more structure, since for each point they add one equation and at least four more parameters.)

Also note that the risk factor x and its disturbance terms are absorbed into the "cyclical" error term ϵ_t^{cyc}, and we assume that the error term follows an AR(1) processes of the form

$$\epsilon_{t+1}^{cyc} = \rho_y \epsilon_t^{cyc} + e_{t+1}^{cyc}, \qquad e_{t+1}^{cyc} \sim N(0, \sigma_{cyc}^2). \tag{27}$$

Now let g_t denote trend real GDP growth. We also treat this variable as observable conditional on time t, set equal to the as-of-date, rolling, exogenously detrended rate of real GDP growth using a Hodrick-Prescott filter. To avoid forward-looking bias, the filter is recalculated for each date in which the natural rate model is computed, so the only r_t^* estimate that contains the full sample information about realized output growth is the last point in the sample.

We then define the state variable z_t as a "headwinds" factor related to the natural rate through the state transition equation

$$r_t^* = z_t + g_t, \tag{28}$$

as is standard in state-space models of the natural rate, such as Laubach and Williams (2003), with the coefficient on growth set to $c = 1$ as above.

Finally, we also assume that the headwinds factor follows an AR(1) process, so that

$$z_{t+1} = \rho_z z_t + e_{t+1}^z, \qquad e_{t+1}^z \sim N(0, \sigma_z^2). \tag{29}$$

Again, we stress why we we see this not just as a macro-finance model, but also the minimal such model we could set up that contains both yields and macro data. The key finance part is the underlying term-structure model of the yield curve. The key macro part is just $r^* = z + g$, which would be meaningless without constraints on z but is disciplined through our assumptions (volatility priors). This will allow us to generate a "feasible" path for r^*, tied in to both the macro and finance blocks, but with little theoretical baggage otherwise.

Thus, including an equation linking r_t^* to yield curve data, Equation 26, and one linking r_t^* to growth, Equation 28, is a distinctive feature of our unified empirical macro-finance model, as we bring information from both financial and macroeconomic data to bear on estimating the natural rate. Consistent with the relative frequencies of financial series and macroeconomic series, the headwinds factor, z_{t+1}, is conjectured to capture structural macroeconomic phenomena with a frequency similar to that of macroeconomic series, while the error to average yields, ϵ_{t+1}^{cyc}, is assumed to capture high frequency movements from financial phenomena. Through Equation 28 this implies a view of the natural rate r_t^* consistent with Laubach and Williams (2003) of representing a medium-run real rate "anchor" for monetary policy. In Appendix A we provide details on how explicit identification assumptions about ρ_z and σ_z prevent the headwinds variable from taking a high frequency similar to that of financial prices. We use priors to impose this view on variable volatility, without explicitly linking the headwinds factor to a particular set of low frequency structural data.

Summarizing the state-space model, the Kalman system is thus defined by the following state equation,

$$\begin{pmatrix} z_t \\ \epsilon_t^{cyc} \end{pmatrix} = \begin{pmatrix} \rho_z & 0 \\ 0 & \rho_{cyc} \end{pmatrix} \begin{pmatrix} z_{t-1} \\ \epsilon_{t-1}^{cyc} \end{pmatrix} + \begin{pmatrix} e_t^z \\ e_t^{cyc} \end{pmatrix} . \tag{30}$$

The associated measurement equation can then be written as

$$\bar{y}_t = a_y + b_\pi \pi_t^* + b_{r^*} g_t + b_{r^*} z_t + \epsilon_t^{cyc} . \tag{31}$$

This fully describes the state-space model, which has then to be estimated. The estimation algorithm is described in Appendix A.

5. Data for estimation and evaluation

Estimation and model evaluation lead us to collect bond data for 10 advanced countries for a maximal sample over the postwar period. The data requirements are as follows, and prompted us to collect data over two different windows, a broad window and a narrow window.

Estimation and evaluation: narrow window using full zero-coupon curves Estimation uses the measurement affine equation $\bar{y}_t = a_y + b_\pi \pi_t^* + b_{r^*} g_t + b_{r^*} z_t + \epsilon_t^{cyc}$. In samples where we have complete information on the zero-coupon yield curve we can construct a true average yield based on 1 to 15 year maturity zero-coupon yields. We also need the more easily sourced data on the rate of output growth (g_t) and the inflation trend (π_t^*, computed via constant-gain learning),.

We refer to these samples as the *narrow window*, and to evaluate the model we calculate the fit of affine equations for yields and returns (or equations derived therefrom), $y_t^{(n)} = A_n + B_n' F_t$ and $rx_{t+1}^{(n)} = \mathfrak{B}_n' F_t + v_t^n$. Specifically we examine yields (at various maturities, 5, 10, and 15 years) as well as average excess returns (averaged over maturities 2 to 180 months, and computed with inverse-maturity weights).

Estimation and evaluation: broad window using proxy average yields Estimation uses the measurement affine equation $\bar{y}_t = a_y + b_\pi \pi^*_t + b_{r^*} g_t + b_{r^*} z_t + \epsilon^{cyc}_t$. Given data on the rate of output growth and the inflation trend, this step can still be carried through in samples where we have an acceptable proxy of average yields, and we lack the zero-coupon yield curve.

We refer to these samples as the *broad window*, where we achieve an estimate of the latent natural rate r^*_t. Also in this case to evaluate the model we can still examine the fit of the affine equations for excess returns, $rx^{(n)}_{t+1} = \mathfrak{B}'_n F_t + v^n_t$, but without the zero-coupon yield curve we need to rely on a proxy measure of excess returns as detailed below.

Whilst this broad window method may give less precise estimates of the natural rate, we find strong correlations between our proxies for yields and returns and their values computed using complete information on the zero-coupon yield curve where the methods overlap in the narrow window. Still, one virtue is that we can compute natural rates often for an extra 10 or 20 years going back to the 1950s and 1960s for the countries in our sample. A second important virtue is that the longer samples provided by this proxy method allow us to achieve more stable estimates of the latent variables by the time the starting point of the narrow window is reached, pushing back the period of initialization where the filter can produce unstable and unreliable estimates (we typically drop the first 5 years a a burn-in period in results shown below).

Data: narrow window In the narrow window samples we need complete information on the zero-coupon yield curve. We use yields at all monthly maturities from 1 to 180 months in all countries. We rely here on existing datasets by official institutions and other researchers.

We employ a Svensson (1994) model of the zero-coupon yield curve. Here a set of time-varying parameters $\beta_{0,t}, \beta_{1,t}, \beta_{2,t}, \beta_{3,t}, \tau_{1,t}$, and $\tau_{2,t}$ are estimated to express the smoothly-approximated yield $y^{(n)}_t$, at any given time t, of a maturity n zero-coupon bond as

$$y^{(n)}_t = \beta_{0,t} + \beta_{1,t} \frac{1 - e^{-n/\tau_{1,t}}}{n/\tau_{1,t}} + \beta_{2,t} \left(\frac{1 - e^{-n/\tau_{1,t}}}{n/\tau_{1,t}} - e^{-n/\tau_{1,t}} \right) + \beta_{3,t} \left(\frac{1 - e^{-n/\tau_{2,t}}}{n/\tau_{2,t}} - e^{-n/\tau_{2,t}} \right) . \tag{32}$$

Obtaining the parameters of a Svensson model lets us generate zero-coupon yields for all maturities at each point in time, circumventing the problem of data sparsity in some parts of the curve. For some countries, the datasets by official institutions and other researchers already provide estimates of the above parameters; we can then directly compute the zero-coupon yields at each date as above without any further step. In other cases, the datasets available to us consist of zero-coupon yields at a large number (but maybe not all) maturities, and possibly build from alternative models, and in these cases we simply fit a Svensson curve as a preliminary step at each date.

For the 10 countries our sources for these fitted Svensson zero-coupon yield curves are as follows:

- U.S.: parameters from Gürkaynak, Sack, and Wright (2007) from June 1961 to the present.
- Japan: yields from the Ministry of Finance starting in September 1974, at maturities from 1 to 40 years.

- Germany: parameters from the Bundesbank from October 1972 to the present.
- U.K.: Bank of England data on yields, allowing us to recover complete yield curves from January 1970 to the present.
- Canada: Bank of Canada estimates of yield curves for maturities ranging from 0.25 years to 30 years from January 1986 to the present.
- Australia: Reserve Bank of Australia data on yields from 0 to 10 years in quarterly maturity increments from July 1992 to the present.
- France: up to 2004 yield curves kindly supplied by Cadorel (2022), at maturities from 1 to 40 years; from 2005, yield curves at maturities from 1 to 50 years, from Grishchenko, Moraux, and Pakulyak (2020) and subsequent updates.
- Spain: parameters kindly supplied by the BIS to construct yield curves from January 1991 to June 2019 (with permission granted to use and share these derived curves).
- Sweden: parameters from the Riksbank from December 1992 to the present.
- Switzerland: parameters from the Swiss National Bank from January 1988 to the present.

To the best of our knowledge, these estimations provide a new and unique set of zero-coupon data unmatched in the literature by extending the Gürkaynak, Sack, and Wright (2007) methodology consistently to other developed markets and over many more years.[8]

Data: broad window As we have seen above, the availability of complete zero-coupon yield curves varies from country to country. We have full coverage for all 10 countries in the last three decades, since roughly the early 1990s. In contrast, for most the 1970s and 1980s only a handful of countries can be covered. For the 1960s, only the U.S. is available.

How then can we estimate the model and, thus, the natural rate outside these windows? As noted, we can use proxies ($\tilde{y}_t$ and $\tilde{y}_t^{(1)}$) to approximate average yields and short rates, and given those proxies, and without a curve, we can approximate average excess bond returns ($\widetilde{rx}_t = \tilde{y}_t - k\tilde{y}_{t+1} - (1-k)y_t^{(1)}$), where the average is over bonds of maturities from 2 to 15 years.[9]

We therefore rely on an array of secondary sources for proxy average yields and short rates. These will typically reference an average built from a vaguely defined basket of long bonds, or will

[8]The closest prior work was a decade ago. Wright (2011) compiled a 10-country panel of zero-coupon yields with the data series ending in 2009, using Svensson, Nelson-Siegel, and spline models.

[9]Consider an inverse-duration weight basket of bonds at annual maturity increments $n = 2, \ldots, 15$. The forward excess return of the maturity n bond is $ny_t^{(n)} - (n-1)y_{t+1}^{(n-1)} - y_t^{(1)}$. Applying a weight $1/n$ and summing over all 14 bonds we obtain a weighted average return $\overline{rx}_t = \frac{1}{14}\sum_{n=2}^{15} y_t^{(n)} - \frac{1}{14}\sum_{n=2}^{15}\frac{(n-1)}{n} y_{t+1}^{(n-1)} - \frac{1}{14}\sum_{n=2}^{15}\frac{1}{n}y_t^{(1)}$. We take the approximation to this given by $\widetilde{rx}_t = \tilde{y}_t - \left(\frac{1}{14}\sum_{n=2}^{15}\frac{(n-1)}{n}\right)\tilde{y}_{t+1} - \left(\frac{1}{14}\sum_{n=2}^{15}\frac{1}{n}\right)y_t^{(1)}$. Now define $k \equiv \left(\frac{1}{14}\sum_{n=2}^{15}\frac{(n-1)}{n}\right)$ and we can write $\widetilde{rx}_t = \tilde{y}_t - k\tilde{y}_{t+1} - (1-k)y_t^{(1)}$.

present a time series of multiple long bond yields from which we can mechanically construct an average. Sources used here include technical documents from central banks and finance ministries, or from the OECD, and aggregators such as Global Financial Data and Haver. A full description of these sources can be found in the online appendix. **[TBD]**

6. Estimates and fit of yield and return equations

6.1. Bond yield regressions

In this subsection, we now apply the affine bond pricing model with OLS regressions based on Equation 11, $y_t^{(n)} = \mathcal{A}_n + \mathcal{B}_n^r r_t^* + \mathcal{B}_n^\pi \pi_t^* + \mathcal{B}^{\bar{c}} \bar{c}_t$. This is the specification in Cieslak and Povala (2015), but with a second trend for the estimated natural rate. The detrended average yield then represents a cyclical fluctuation of bond yields (or prices) about the long run trends. We could also run this regression in equivalent form with $\bar{c}_t$ replaced by $\bar{y}_t$, but this would only produce different coefficients requiring a different interpretation or attribution, but the model and fit would be the same.

Our findings confirm and extend those of Cieslak and Povala (2015), in two ways. First, the inclusion of the inflation trend improves the fit of the yield model relative to a specification with no trends. Second, this is true for all 10 advanced economies and not just the U.S., and notably, the fit improvement is most marked at the longer end of the curve. Third, the inclusion of the natural rate trend improves the fit even more, confirming that both trends are relevant for bond pricing, as in Bauer and Rudebusch (2020).

Table 1 presents full-sample OLS yield regressions at the 5-year maturity point. Panel (a) uses the average yield as the only factor. Panel (b) uses the average yield and the inflation trend only, where the average yield is first detrended. Panel (c) uses the average yield and both trends, where the average yield is first detrended. In this case, at the shorter end of the curve, the improvements in fit are small as we move from the first specification to the second and then the third. And, as is generally seen in the literature, the fit is always very close to an R^2 of 1.

Table 2 presents OLS yield regressions at the 10-year maturity point and Table 3 presents OLS yield regressions at the 15-year maturity point. Here, the improvements in fit are a little more evident, but we start from a very high baseline fit in the yields-only specification so these increments can only be quite small.

Of greater interest, as highlighted by Cieslak and Povala (2015), is the role of the trends versus the cyclical detrended yield term in accounting for the fit. This is shown in Table 4 and the result is striking. Here the R^2 measures are typically around 90% of those seen in the previous tables, indicating that when it comes to explaining the level of yields, the macro trends are doing almost all of the work, and that the orthogonal component of yields $\bar{c}$ only accounts for around 10% of the fit. Indeed, complementary regressions (not shown) including only the detrended yields $\bar{c}$ show this to be the case.

Table 1: *International yields, 5-year maturity*

The tables reports OLS estimates on international monthly data of yields $y_t^{(n)} = \tilde{\mathcal{A}}_n + \tilde{\mathcal{B}}^{\bar{c}}\bar{c}_t$. * $p < 0.05$, ** $p < 0.01$, *** $p < 0.001$. The sample varies by country.

(a) Narrow window. Detrending: none.

	(1) AUS	(2) CAN	(3) CHE	(4) DEU	(5) ESP	(6) FRA	(7) GBR	(8) JPN	(9) SWE	(10) USA
$\bar{y}$	1.059***	1.011***	1.024***	1.043***	1.062***	0.988***	1.011***	1.025***	1.012***	1.045***
	(0.003)	(0.002)	(0.003)	(0.002)	(0.003)	(0.004)	(0.003)	(0.002)	(0.003)	(0.002)
Constant	-0.004***	-0.003***	-0.003***	-0.004***	-0.006***	-0.004***	-0.002***	-0.003***	-0.003***	-0.005***
	(0.000)	(0.000)	(0.000)	(0.000)	(0.000)	(0.000)	(0.000)	(0.000)	(0.000)	(0.000)
Observations	354	432	408	591	342	561	624	553	349	634
R^2	0.997	0.998	0.997	0.997	0.998	0.991	0.993	0.997	0.998	0.997
RSS	0.0007	0.0009	0.0005	0.0020	0.0008	0.0074	0.0071	0.0016	0.0006	0.0022

(b) Narrow window. Detrending: inflation only, $\bar{c}$ equal to projection of $\bar{y}$ on π.

	(1) AUS	(2) CAN	(3) CHE	(4) DEU	(5) ESP	(6) FRA	(7) GBR	(8) JPN	(9) SWE	(10) USA
π^*	2.258***	1.683***	1.672***	1.963***	1.809***	0.997***	0.935***	0.900***	1.620***	1.464***
	(0.009)	(0.005)	(0.005)	(0.006)	(0.005)	(0.005)	(0.003)	(0.002)	(0.004)	(0.004)
$c^{(\pi^*)}$	1.060***	1.020***	1.042***	1.042***	1.052***	1.014***	1.045***	1.004***	1.058***	1.071***
	(0.005)	(0.004)	(0.007)	(0.004)	(0.009)	(0.009)	(0.007)	(0.005)	(0.004)	(0.005)
Constant	-0.015***	0.001***	-0.002***	-0.003***	-0.015***	0.010***	0.018***	0.010***	0.001***	-0.000
	(0.000)	(0.000)	(0.000)	(0.000)	(0.000)	(0.000)	(0.000)	(0.000)	(0.000)	(0.000)
Observations	354	432	408	591	342	561	624	553	349	634
R^2	0.997	0.998	0.997	0.997	0.998	0.991	0.994	0.997	0.999	0.997
RSS	0.0007	0.0009	0.0005	0.0020	0.0008	0.0072	0.0067	0.0016	0.0004	0.0021

(c) Narrow window. Detrending: inflation and natural rate, $\bar{c}$ equal to projection of $\bar{y}$ on π^* and r^* .

	(1) AUS	(2) CAN	(3) CHE	(4) DEU	(5) ESP	(6) FRA	(7) GBR	(8) JPN	(9) SWE	(10) USA
π^*	1.030***	0.985***	1.154***	0.937***	1.317***	0.979***	0.641***	0.461***	0.926***	1.119***
	(0.011)	(0.005)	(0.006)	(0.007)	(0.021)	(0.004)	(0.004)	(0.003)	(0.005)	(0.004)
r^*	1.271***	1.161***	1.380***	1.640***	0.592***	1.126***	1.514***	0.754***	1.006***	1.193***
	(0.006)	(0.005)	(0.011)	(0.007)	(0.025)	(0.012)	(0.011)	(0.004)	(0.004)	(0.008)
$c^{(\pi^*,r^*)}$	1.014***	1.099***	1.080***	1.092***	1.063***	1.063***	0.987***	1.049***	1.070***	1.079***
	(0.011)	(0.009)	(0.014)	(0.008)	(0.009)	(0.019)	(0.010)	(0.010)	(0.008)	(0.008)
Constant	-0.005***	-0.006***	-0.003***	-0.004***	-0.011***	-0.007***	-0.009***	-0.006***	-0.001***	-0.007***
	(0.000)	(0.000)	(0.000)	(0.000)	(0.000)	(0.000)	(0.000)	(0.000)	(0.000)	(0.000)
Observations	354	432	408	591	342	561	624	553	349	634
R^2	0.997	0.998	0.997	0.997	0.998	0.991	0.994	0.997	0.999	0.997
RSS	0.0007	0.0007	0.0005	0.0018	0.0008	0.0071	0.0062	0.0015	0.0004	0.0021

Table 2: *International yields, 10-year maturity*

The tables reports OLS estimates on international monthly data of yields $y_t^{(n)} = \tilde{\mathcal{A}}_n + \tilde{\mathcal{B}}^{\bar{c}}\bar{c}_t$. * $p < 0.05$, ** $p < 0.01$, *** $p < 0.001$. The sample varies by country.

(a) Narrow window. Detrending: none.

	(1) AUS	(2) CAN	(3) CHE	(4) DEU	(5) ESP	(6) FRA	(7) GBR	(8) JPN	(9) SWE	(10) USA
$\bar{y}$	1.000***	0.988***	0.965***	0.984***	0.949***	0.996***	0.997***	0.985***	1.006***	0.959***
	(0.004)	(0.003)	(0.004)	(0.003)	(0.004)	(0.003)	(0.003)	(0.002)	(0.003)	(0.003)
Constant	0.002***	0.003***	0.003***	0.004***	0.006***	0.004***	0.002***	0.003***	0.003***	0.005***
	(0.000)	(0.000)	(0.000)	(0.000)	(0.000)	(0.000)	(0.000)	(0.000)	(0.000)	(0.000)
Observations	354	432	408	591	342	561	624	553	349	634
R^2	0.995	0.995	0.992	0.993	0.995	0.994	0.994	0.996	0.997	0.993
RSS	0.0009	0.0019	0.0014	0.0036	0.0015	0.0050	0.0057	0.0017	0.0007	0.0039

(b) Narrow window. Detrending: inflation only, $\bar{c}$ equal to projection of $\bar{y}$ on π.

	(1) AUS	(2) CAN	(3) CHE	(4) DEU	(5) ESP	(6) FRA	(7) GBR	(8) JPN	(9) SWE	(10) USA
π^*	2.178***	1.640***	1.591***	1.872***	1.598***	1.019***	0.945***	0.858***	1.648***	1.360***
	(0.010)	(0.007)	(0.008)	(0.008)	(0.006)	(0.004)	(0.003)	(0.002)	(0.005)	(0.005)
$c^{(\pi^*)}$	0.971***	1.008***	0.927***	0.966***	1.032***	0.963***	0.954***	0.993***	0.993***	0.930***
	(0.005)	(0.006)	(0.012)	(0.005)	(0.011)	(0.008)	(0.006)	(0.005)	(0.005)	(0.007)
Constant	-0.010***	0.007***	0.004***	0.005***	-0.002***	0.018***	0.021***	0.015***	0.005***	0.009***
	(0.000)	(0.000)	(0.000)	(0.000)	(0.000)	(0.000)	(0.000)	(0.000)	(0.000)	(0.000)
Observations	354	432	408	591	342	561	624	553	349	634
R^2	0.996	0.995	0.992	0.994	0.996	0.994	0.995	0.997	0.997	0.993
RSS	0.0008	0.0019	0.0013	0.0035	0.0012	0.0048	0.0051	0.0017	0.0007	0.0038

(c) Narrow window. Detrending: inflation and natural rate, $\bar{c}$ equal to projection of $\bar{y}$ on π^* and r^*.

	(1) AUS	(2) CAN	(3) CHE	(4) DEU	(5) ESP	(6) FRA	(7) GBR	(8) JPN	(9) SWE	(10) USA
π^*	1.058***	0.920***	1.104***	0.877***	0.886***	1.002***	0.689***	0.404***	0.990***	1.047***
	(0.012)	(0.008)	(0.010)	(0.009)	(0.027)	(0.004)	(0.004)	(0.003)	(0.007)	(0.006)
r^*	1.159***	1.197***	1.297***	1.590***	0.858***	1.109***	1.316***	0.778***	0.954***	1.082***
	(0.007)	(0.008)	(0.017)	(0.009)	(0.031)	(0.009)	(0.010)	(0.004)	(0.005)	(0.011)
$c^{(\pi^*,r^*)}$	0.948***	0.912***	0.812***	0.869***	1.020***	0.892***	0.983***	0.882***	0.969***	0.889***
	(0.012)	(0.014)	(0.022)	(0.010)	(0.011)	(0.015)	(0.009)	(0.010)	(0.011)	(0.011)
Constant	-0.001*	0.000	0.003***	0.003***	0.005***	0.000	-0.003***	-0.001***	0.003***	0.002***
	(0.000)	(0.000)	(0.000)	(0.000)	(0.000)	(0.000)	(0.000)	(0.000)	(0.000)	(0.000)
Observations	354	432	408	591	342	561	624	553	349	634
R^2	0.996	0.996	0.993	0.995	0.996	0.994	0.995	0.997	0.997	0.994
RSS	0.0008	0.0017	0.0012	0.0028	0.0012	0.0046	0.0049	0.0013	0.0007	0.0036

Table 3: *International yields, 15-year maturity*

The tables reports OLS estimates on international monthly data of yields $y_t^{(n)} = \tilde{\mathcal{A}}_n + \tilde{\mathcal{B}}^{\bar{c}}\bar{c}_t$. * $p < 0.05$, ** $p < 0.01$, *** $p < 0.001$. The sample varies by country.

(a) Narrow window. Detrending: none.

$\bar{y}$	0.923***	0.964***	0.936***	0.934***	0.875***	0.988***	0.978***	0.948***	0.987***	0.916***
	(0.007)	(0.006)	(0.008)	(0.006)	(0.006)	(0.007)	(0.008)	(0.005)	(0.005)	(0.005)
Constant	0.006***	0.007***	0.006***	0.009***	0.013***	0.008***	0.005***	0.006***	0.006***	0.010***
	(0.000)	(0.000)	(0.000)	(0.000)	(0.000)	(0.000)	(0.001)	(0.000)	(0.000)	(0.000)
Observations	354	432	408	591	342	561	624	553	349	634
R^2	0.982	0.984	0.974	0.977	0.987	0.976	0.962	0.982	0.991	0.979
RSS	0.0031	0.0057	0.0041	0.0112	0.0032	0.0191	0.0388	0.0081	0.0025	0.0112

(b) Narrow window. Detrending: inflation only, $\bar{c}$ equal to projection of $\bar{y}$ on π.

	(1) AUS	(2) CAN	(3) CHE	(4) DEU	(5) ESP	(6) FRA	(7) GBR	(8) JPN	(9) SWE	(10) USA
π^*	2.014***	1.606***	1.548***	1.783***	1.469***	1.015***	0.940***	0.815***	1.644***	1.310***
	(0.018)	(0.012)	(0.013)	(0.014)	(0.009)	(0.007)	(0.008)	(0.005)	(0.009)	(0.008)
$c^{(\pi^*)}$	0.893***	0.972***	0.880***	0.912***	0.977***	0.942***	0.896***	0.993***	0.937***	0.852***
	(0.010)	(0.011)	(0.020)	(0.009)	(0.017)	(0.015)	(0.015)	(0.011)	(0.009)	(0.012)
Constant	-0.005***	0.010***	0.007***	0.009***	0.006***	0.022***	0.023***	0.019***	0.008***	0.013***
	(0.001)	(0.000)	(0.000)	(0.000)	(0.000)	(0.000)	(0.001)	(0.000)	(0.000)	(0.000)
Observations	354	432	408	591	342	561	624	553	349	634
R^2	0.983	0.984	0.975	0.978	0.988	0.977	0.964	0.983	0.992	0.980
RSS	0.0029	0.0057	0.0040	0.0110	0.0029	0.0187	0.0365	0.0078	0.0022	0.0106

(c) Narrow window. Detrending: inflation and natural rate, $\bar{c}$ equal to projection of $\bar{y}$ on π^* and r^* .

	(1) AUS	(2) CAN	(3) CHE	(4) DEU	(5) ESP	(6) FRA	(7) GBR	(8) JPN	(9) SWE	(10) USA
π^*	1.010***	0.889***	1.065***	0.820***	0.707***	0.998***	0.713***	0.361***	1.025***	1.015***
	(0.022)	(0.013)	(0.017)	(0.016)	(0.040)	(0.007)	(0.009)	(0.007)	(0.012)	(0.010)
r^*	1.040***	1.192***	1.287***	1.540***	0.918***	1.095***	1.170***	0.778***	0.897***	1.021***
	(0.013)	(0.013)	(0.030)	(0.015)	(0.047)	(0.019)	(0.026)	(0.009)	(0.010)	(0.018)
$c^{(\pi^*,r^*)}$	0.959***	0.754***	0.648***	0.740***	0.957***	0.843***	1.007***	0.882***	0.924***	0.782***
	(0.022)	(0.022)	(0.038)	(0.018)	(0.016)	(0.030)	(0.025)	(0.023)	(0.020)	(0.018)
Constant	0.003***	0.004***	0.006***	0.008***	0.012***	0.005***	0.002*	0.002***	0.006***	0.007***
	(0.001)	(0.000)	(0.000)	(0.000)	(0.000)	(0.000)	(0.001)	(0.000)	(0.000)	(0.000)
Observations	354	432	408	591	342	561	624	553	349	634
R^2	0.983	0.988	0.978	0.982	0.989	0.977	0.966	0.984	0.992	0.981
RSS	0.0028	0.0045	0.0036	0.0091	0.0027	0.0182	0.0348	0.0074	0.0022	0.0102

Table 4: *International yields, contribution of macro trends alone*

The tables reports OLS estimates on international monthly data of yields $y_t^{(n)} = \tilde{\mathcal{A}}_n + \tilde{\mathcal{B}}^{\bar{c}} \bar{c}_t$. * $p < 0.05$, ** $p < 0.01$, *** $p < 0.001$. The sample varies by country.

(a) Narrow window. 5-year yields regressed on π^* and r^* alone .

	(1) AUS	(2) CAN	(3) CHE	(4) DEU	(5) ESP	(6) FRA	(7) GBR	(8) JPN	(9) SWE	(10) USA
π^*	1.030***	0.985***	1.154***	0.937***	1.317***	0.979***	0.641***	0.461***	0.926***	1.119***
	(0.055)	(0.031)	(0.025)	(0.041)	(0.144)	(0.012)	(0.016)	(0.015)	(0.034)	(0.023)
r^*	1.271***	1.161***	1.380***	1.640***	0.592***	1.126***	1.514***	0.754***	1.006***	1.193***
	(0.033)	(0.031)	(0.044)	(0.040)	(0.169)	(0.030)	(0.043)	(0.018)	(0.029)	(0.045)
Constant	-0.005***	-0.006***	-0.003***	-0.004***	-0.011***	-0.007***	-0.009***	-0.006***	-0.001*	-0.007***
	(0.001)	(0.001)	(0.000)	(0.001)	(0.002)	(0.001)	(0.001)	(0.001)	(0.001)	(0.001)
Observations	354	432	408	591	342	561	624	553	349	634
R^2	0.920	0.933	0.958	0.899	0.904	0.940	0.909	0.944	0.929	0.910
RSS	0.0179	0.0261	0.0077	0.0614	0.0340	0.0476	0.0960	0.0293	0.0195	0.0607

(b) Narrow window. 10-year yields regressed on π^* and r^* alone .

	(1) AUS	(2) CAN	(3) CHE	(4) DEU	(5) ESP	(6) FRA	(7) GBR	(8) JPN	(9) SWE	(10) USA
π^*	1.058***	0.920***	1.104***	0.877***	0.886***	1.002***	0.689***	0.404***	0.990***	1.047***
	(0.052)	(0.027)	(0.020)	(0.034)	(0.139)	(0.010)	(0.015)	(0.013)	(0.032)	(0.020)
r^*	1.159***	1.197***	1.297***	1.590***	0.858***	1.109***	1.316***	0.778***	0.954***	1.082***
	(0.031)	(0.027)	(0.036)	(0.033)	(0.164)	(0.025)	(0.043)	(0.015)	(0.026)	(0.038)
Constant	-0.001	0.000	0.003***	0.003***	0.005**	0.000	-0.003*	-0.001**	0.003***	0.002**
	(0.001)	(0.001)	(0.000)	(0.001)	(0.002)	(0.001)	(0.001)	(0.000)	(0.001)	(0.001)
Observations	354	432	408	591	342	561	624	553	349	634
R^2	0.920	0.949	0.968	0.925	0.888	0.959	0.909	0.956	0.940	0.924
RSS	0.0159	0.0192	0.0053	0.0406	0.0318	0.0331	0.0939	0.0209	0.0164	0.0435

(c) Narrow window. 15-year yields regressed on π^* and r^* alone .

	(1) AUS	(2) CAN	(3) CHE	(4) DEU	(5) ESP	(6) FRA	(7) GBR	(8) JPN	(9) SWE	(10) USA
π^*	1.010***	0.889***	1.065***	0.820***	0.707***	0.998***	0.713***	0.361***	1.025***	1.015***
	(0.056)	(0.025)	(0.022)	(0.032)	(0.135)	(0.011)	(0.018)	(0.014)	(0.032)	(0.019)
r^*	1.040***	1.192***	1.287***	1.540***	0.918***	1.095***	1.170***	0.778***	0.897***	1.021***
	(0.034)	(0.025)	(0.039)	(0.031)	(0.158)	(0.029)	(0.050)	(0.018)	(0.026)	(0.037)
Constant	0.003*	0.004***	0.006***	0.008***	0.012***	0.005***	0.002	0.002***	0.006***	0.007***
	(0.001)	(0.001)	(0.000)	(0.001)	(0.002)	(0.001)	(0.001)	(0.001)	(0.001)	(0.001)
Observations	354	432	408	591	342	561	624	553	349	634
R^2	0.894	0.954	0.961	0.927	0.878	0.946	0.875	0.940	0.938	0.922
RSS	0.0183	0.0164	0.0062	0.0365	0.0296	0.0437	0.1281	0.0271	0.0165	0.0410

6.2. Excess return regressions

We just saw that macro trends can improve the modeling of yields, but we now see how they matter for predicting bond returns. Similar findings were shown for the U.S. case in Cieslak and Povala (2015) with just an inflation trend, and also in the contemporaneous work of Bauer and Rudebusch (2020) with trends for inflation and the natural rate combined. We show that the same applies more generally at the international level for both yields and excess returns.

The intuition is quite straightforward. The macro trend factors, being slow moving and near unit-root, are mainly priced in one-period ahead and, being so highly persistent, they contain little new useful information about short-run returns. In contrast, the cyclical factor, being the more volatile driver of the high-frequency error-correction part of the bond price process, is very much more informative about how bond prices revert to trend in the short run.

Formally, in this section we present estimates for the excess return Equation 13, $rx_{t+1}^{(n)} = \mathfrak{B}_n^\top F_t + v_t^n$. These one-step ahead predictions are noisy but their explanatory power is almost entirely due to the role of the detrended, or cyclical, yield factor $\bar{c}$. This is inline with intuition, and the cyclical factor is the only force at work in the long-maturity limit, as we saw at Equation 25.

Table 5 present results for the excess return forecasts in the narrow window sample. Here we have full zero-coupon yield curves and do not have to rely on proxy yields or proxy returns. Note that these are in-sample regressions (using 2-sided r^* estimates) and, whilst illustrative, they should not be judged the same as real-time out-of-sample forecasts, which we discuss below. As is clear, when we move from a yields only model in panel (a), to the model with the inflation trend in panel (b) and then the two trends in panel (c), the fit of the excess return forecasts improves dramatically. For the U.S., the R^2 rises from 0.004, to 0.128, to 0.207; and the RSS falls from 0.0624, to 0.0546, to 0.0497. Similar large improvements are seen across all 10 countries, though from different baselines.

Table 6 recasts the regressions with two trends in panel (a), but here replacing the detrended yield $\bar{c}$ with the average yield itself $\bar{y}$. This allows a different interpretation and a sense check. Holding fixed the average level of yields we would expect increases in either macro trend (higher inflation or higher natural rates) to be associated with lower returns (bond prices adjusting down) going forward, and this intuition is confirmed, and 19 of 20 trend coefficients are negative in this panel (the only exception is not statistically significant). Panel (b) allows for a different check, and recasts the regressions with two trends but now excluding the average yield term. This amounts to omitting the detrending, and our intuition above was that this should destroy the fit of the forecast since the volatile cyclical term is the main source of predictive power, and this is indeed the case. The fit here is 80%-90% attenuated relative to the fit achieved when the cyclical term is present.

Table 7 expands the sample to the broad window, to see if similar success is achieved with yield and return proxies in periods when the full curve is not available. Despite the noisier data, the fit of the full model in panel (a) remains good (all 20 trend coefficients are negative) even for countries with large spans of proxy information. And in panel (b) the intuition about detrending is preserved, and macro trends alone still account for only a small share of the forecasts' explanatory power.

Table 5: *International excess returns, weighted-average portfolio*

The table reports OLS estimates on international data of the excess return equation $rx_{t+1}^{(n)} = \mathfrak{B}_n^\top F_t + v_t^n$. * $p < 0.05$, ** $p < 0.01$, *** $p < 0.001$. The sample varies by country.

(a) Narrow window. Detrending: none.

	(1) AUS	(2) CAN	(3) CHE	(4) DEU	(5) ESP	(6) FRA	(7) GBR	(8) JPN	(9) SWE	(10) USA
$\bar{y}$	0.112***	0.031**	0.013	0.025*	0.082***	-0.012	0.019	0.035***	0.097***	0.021
	(0.019)	(0.012)	(0.016)	(0.011)	(0.019)	(0.011)	(0.010)	(0.009)	(0.017)	(0.013)
Constant	-0.002*	0.002**	0.002***	0.002***	0.001	0.003***	0.001	0.002***	0.001	0.002
	(0.001)	(0.001)	(0.000)	(0.001)	(0.001)	(0.001)	(0.001)	(0.000)	(0.001)	(0.001)
Observations	348	426	403	586	330	538	618	547	345	629
R^2	0.090	0.016	0.002	0.008	0.053	0.002	0.006	0.027	0.089	0.004
RSS	0.0241	0.0221	0.0172	0.0402	0.0349	0.0492	0.0636	0.0223	0.0256	0.0624

(b) Narrow window. Detrending: inflation only, $\bar{c}$ equal to projection of $\bar{y}$ on π.

	(1) AUS	(2) CAN	(3) CHE	(4) DEU	(5) ESP	(6) FRA	(7) GBR	(8) JPN	(9) SWE	(10) USA
π^*	0.204***	-0.049*	-0.016	0.041	0.023	-0.050***	0.007	0.004	0.055	-0.045*
	(0.053)	(0.021)	(0.027)	(0.027)	(0.028)	(0.012)	(0.011)	(0.009)	(0.031)	(0.019)
$c^{(\pi^*)}$	0.132***	0.189***	0.152***	0.029	0.654***	0.148***	0.055**	0.132***	0.251***	0.263***
	(0.029)	(0.021)	(0.042)	(0.018)	(0.048)	(0.024)	(0.020)	(0.018)	(0.030)	(0.028)
Constant	-0.002	0.005***	0.002***	0.003**	0.005***	0.004***	0.002**	0.003***	0.003***	0.005***
	(0.002)	(0.001)	(0.000)	(0.001)	(0.001)	(0.001)	(0.001)	(0.000)	(0.001)	(0.001)
Observations	348	426	403	586	330	538	618	547	345	629
R^2	0.092	0.174	0.033	0.008	0.360	0.096	0.012	0.089	0.180	0.128
RSS	0.0241	0.0186	0.0166	0.0402	0.0236	0.0445	0.0632	0.0209	0.0231	0.0546

(c) Narrow window. Detrending: inflation and natural rate, $\bar{c}$ equal to projection of $\bar{y}$ on π^* and r^*.

	(1) AUS	(2) CAN	(3) CHE	(4) DEU	(5) ESP	(6) FRA	(7) GBR	(8) JPN	(9) SWE	(10) USA
π^*	0.232***	-0.122***	0.004	0.080*	-0.439***	-0.051***	0.023	-0.025*	-0.004	-0.066**
	(0.053)	(0.024)	(0.034)	(0.032)	(0.123)	(0.011)	(0.012)	(0.012)	(0.031)	(0.021)
r^*	-0.030	0.124***	-0.054	-0.064*	0.562***	0.077**	-0.085*	0.050***	0.087**	0.074
	(0.033)	(0.025)	(0.060)	(0.032)	(0.146)	(0.030)	(0.034)	(0.015)	(0.027)	(0.041)
$c^{(\pi^*,r^*)}$	0.731***	0.511***	0.710***	0.248***	0.645***	0.399***	0.252***	0.372***	0.831***	0.492***
	(0.053)	(0.042)	(0.076)	(0.036)	(0.050)	(0.047)	(0.032)	(0.037)	(0.053)	(0.040)
Constant	-0.002	0.004***	0.002***	0.003***	0.009***	0.003***	0.004***	0.002***	0.003***	0.004***
	(0.001)	(0.001)	(0.000)	(0.001)	(0.001)	(0.001)	(0.001)	(0.000)	(0.001)	(0.001)
Observations	348	426	403	586	330	538	618	547	345	629
R^2	0.378	0.296	0.182	0.086	0.361	0.156	0.101	0.170	0.434	0.207
RSS	0.0165	0.0158	0.0141	0.0370	0.0235	0.0416	0.0575	0.0190	0.0159	0.0497

Table 6: *International excess returns, additional results, narrow window*

The table reports OLS estimates on international data of the excess return equation $rx_{t+1}^{(n)} = \mathfrak{B}_n^\top F_t + v_t^n$. * $p < 0.05$, ** $p < 0.01$, *** $p < 0.001$. The sample varies by country.

(a) Narrow window. Detrending: inflation and natural rate, without projecting $\bar{y}$.

	(1) AUS	(2) CAN	(3) CHE	(4) DEU	(5) ESP	(6) FRA	(7) GBR	(8) JPN	(9) SWE	(10) USA
π^*	-0.491***	-0.619***	-0.802***	-0.139**	-1.166***	-0.449***	-0.144***	-0.184***	-0.811***	-0.600***
	(0.075)	(0.048)	(0.092)	(0.045)	(0.135)	(0.048)	(0.024)	(0.020)	(0.060)	(0.048)
r^*	-0.898***	-0.470***	-1.012***	-0.459***	0.114	-0.374***	-0.440***	-0.234***	-0.707***	-0.475***
	(0.071)	(0.055)	(0.119)	(0.065)	(0.150)	(0.061)	(0.056)	(0.032)	(0.057)	(0.060)
$\bar{y}$	0.731***	0.511***	0.710***	0.248***	0.645***	0.399***	0.252***	0.372***	0.831***	0.492***
	(0.053)	(0.042)	(0.076)	(0.036)	(0.050)	(0.047)	(0.032)	(0.037)	(0.053)	(0.040)
Constant	-0.001	0.006***	0.002***	0.003***	0.011***	0.004***	0.005***	0.003***	0.002***	0.005***
	(0.001)	(0.001)	(0.000)	(0.001)	(0.002)	(0.001)	(0.001)	(0.000)	(0.001)	(0.001)
Observations	348	426	403	586	330	538	618	547	345	629
R^2	0.378	0.296	0.182	0.086	0.361	0.156	0.101	0.170	0.434	0.207
RSS	0.0165	0.0158	0.0141	0.0370	0.0235	0.0416	0.0575	0.0190	0.0159	0.0497

(b) Narrow window. Macro trends only.

	(1) AUS	(2) CAN	(3) CHE	(4) DEU	(5) ESP	(6) FRA	(7) GBR	(8) JPN	(9) SWE	(10) USA
π^*	0.232***	-0.122***	0.004	0.080*	-0.439**	-0.051***	0.023	-0.025	-0.004	-0.066**
	(0.066)	(0.028)	(0.037)	(0.034)	(0.152)	(0.012)	(0.013)	(0.013)	(0.041)	(0.024)
r^*	-0.030	0.124***	-0.054	-0.064	0.562**	0.077*	-0.085*	0.050**	0.087*	0.074
	(0.040)	(0.029)	(0.066)	(0.033)	(0.180)	(0.032)	(0.036)	(0.016)	(0.035)	(0.046)
Constant	-0.002	0.004***	0.002***	0.003***	0.009***	0.003***	0.004***	0.002***	0.003***	0.004***
	(0.002)	(0.001)	(0.001)	(0.001)	(0.002)	(0.001)	(0.001)	(0.000)	(0.001)	(0.001)
Observations	348	426	403	586	330	538	618	547	345	629
R^2	0.040	0.052	0.002	0.010	0.030	0.042	0.010	0.018	0.025	0.012
RSS	0.0254	0.0213	0.0172	0.0401	0.0358	0.0472	0.0634	0.0225	0.0274	0.0619

Table 7: *International excess returns, additional results, broad window*

The table reports OLS estimates on international data of the excess return equation $rx_{t+1}^{(n)} = \mathfrak{B}_n^{\top} F_t + v_t^n$. * $p < 0.05$, ** $p < 0.01$, *** $p < 0.001$. The sample varies by country.

(a) Broad window. Detrending: inflation and natural rate, without projecting $\bar{y}$.

	(1) AUS	(2) CAN	(3) CHE	(4) DEU	(5) ESP	(6) FRA	(7) GBR	(8) JPN	(9) SWE	(10) USA
π^*	-0.418***	-0.491***	-0.563***	-0.141**	-0.442***	-0.444***	-0.152***	-0.184***	-0.859***	-0.606***
	(0.043)	(0.037)	(0.088)	(0.045)	(0.040)	(0.047)	(0.024)	(0.020)	(0.070)	(0.048)
r^*	-0.252***	-0.546***	-0.649***	-0.559***	-0.492***	-0.344***	-0.414***	-0.229***	-0.661***	-0.469***
	(0.060)	(0.053)	(0.095)	(0.063)	(0.065)	(0.060)	(0.056)	(0.032)	(0.072)	(0.060)
$\bar{y}$	0.343***	0.487***	0.435***	0.282***	0.527***	0.395***	0.258***	0.370***	0.741***	0.497***
	(0.038)	(0.036)	(0.070)	(0.035)	(0.045)	(0.046)	(0.032)	(0.037)	(0.063)	(0.040)
Constant	0.002*	0.003***	0.003***	0.002**	0.004***	0.004***	0.005***	0.003***	0.005***	0.005***
	(0.001)	(0.001)	(0.001)	(0.001)	(0.001)	(0.001)	(0.001)	(0.000)	(0.001)	(0.001)
Observations	622	742	623	634	473	563	634	553	527	634
R^2	0.164	0.203	0.071	0.113	0.233	0.158	0.098	0.170	0.224	0.209
RSS	0.0663	0.0635	0.0351	0.0411	0.0457	0.0431	0.0590	0.0191	0.0759	0.0501

(b) Broad window. Macro trends only.

	(1) AUS	(2) CAN	(3) CHE	(4) DEU	(5) ESP	(6) FRA	(7) GBR	(8) JPN	(9) SWE	(10) USA
π^*	-0.049**	-0.037*	-0.028	0.111***	-0.024	-0.050***	0.017	-0.025	-0.061**	-0.066**
	(0.015)	(0.018)	(0.018)	(0.033)	(0.019)	(0.012)	(0.013)	(0.013)	(0.021)	(0.024)
r^*	0.197***	0.041	-0.112**	-0.113***	0.099*	0.102***	-0.047	0.052**	0.059	0.088
	(0.037)	(0.034)	(0.039)	(0.031)	(0.046)	(0.031)	(0.035)	(0.016)	(0.043)	(0.045)
Constant	0.000	0.002*	0.003***	0.002**	0.003***	0.003**	0.003***	0.002***	0.005***	0.004***
	(0.001)	(0.001)	(0.001)	(0.001)	(0.001)	(0.001)	(0.001)	(0.000)	(0.001)	(0.001)
N	622	742	623	634	473	563	634	553	527	634
R^2	0.052	0.005	0.014	0.025	0.010	0.048	0.004	0.020	0.016	0.013
rss	0.0753	0.0792	0.0372	0.0452	0.0590	0.0487	0.0652	0.0226	0.0961	0.0626

6.3. Model fit: in-sample

To better compare model fit, Figure 4 is based on the yield regressions at the 10-year maturity point in Table 2, and uses the Fields (2003) regression decomposition method for R^2 to attribute contributions of explanatory power to each regressor. As in most affine models, using a contemporaneous yield factor generates a very high R^2, but the figure clarifies the source of this excellent fit. When 0 macro trends are present it is all attributed to the average yield factor $\bar{y}$. But once $\bar{y}$ is detrended using 1 or 2 trends, we find that the macro trends π^* and r^* are responsible for 90% of the empirical fit, and the cyclically-detrended yield factor c_t accounts for only about 10% of the fit. That is to say, over the last 50 years in advanced economies, the level of yields have been consistently explained to a dominant extent by the levels of inflation and natural rate trends.

Figure 5 is based on the excess return regressions for the weighted -average bond portfolio in Table 5, and also uses the Fields (2003) regression decomposition method. When 0 macro trends are present and the only regressor is $\bar{y}$, the fit is poor. But once $\bar{y}$ is detrended using 1 or 2 trends, we find that the fit improves dramatically. With c_t as a regressor alongside the the macro trends π^* and r^*, then again, consistent with intuition grounded in theory, the cyclically-detrended yield factor accounts for over 90% of the fit on average. That is to say, over the last 50 years in advanced economies, excess returns have also been consistently explained to a dominant extent by the levels of cyclically-detrended yields, accounting for the underlying and inflation and natural rate trends. Without accounting for these trends, investors would be misguided as to the deviation of yields from their equilibrium, and would therefore make much poorer predictions of returns.

6.4. Model fit: out-of-sample

The above evidence is based on strictly in-sample metrics of fit. A natural question is whether the use of macro trends also improves out-of-sample fit, which is usually the gold standard for models of return prediction. To that end, for the various excess return forecast regressions we compared in- and out-of-sample fit for the 2010–2019 period.

The choice of period was appealing for three reasons: first, it excludes the pandemic shock; second, it allows sufficient length for every country to have a reasonable size of training period, given that yield curves start only in the 1990s for some countries; third, we expected that both π^* and r^* would have variation in this period, in line with prior work, so this would give both trends to potentially make meaningful contributions to model performance, as compared to periods (like the pre-2008 Great Moderation era) when relative stability of both trends would limit their potential usefulness versus a no-trend model with constant terms implicitly in their stead.

Figure 6 shows the results of this exercise. Model residuals are collected for 10 countries in each period, and the resulting pooled mean squared error, *MSE*, is calculated. The null is the 0-trend model with a yield factor $\bar{y}$. *MSE* ratios are relative to the null. The alternative models add: (I) 1-trend using π^*; (II) 1-trend using r^*; and (III) 2-trends using π^* and r^*.

Figure 4: *Decomposition of in-sample fit: yield regressions with 0, 1, and 2 macro trends*

The chart displays R^2 values for the excess returns regressions by country. 0 denotes the model with no trend, 1 the model with π^* trend, and 2 the model with π^* and r^* trends.

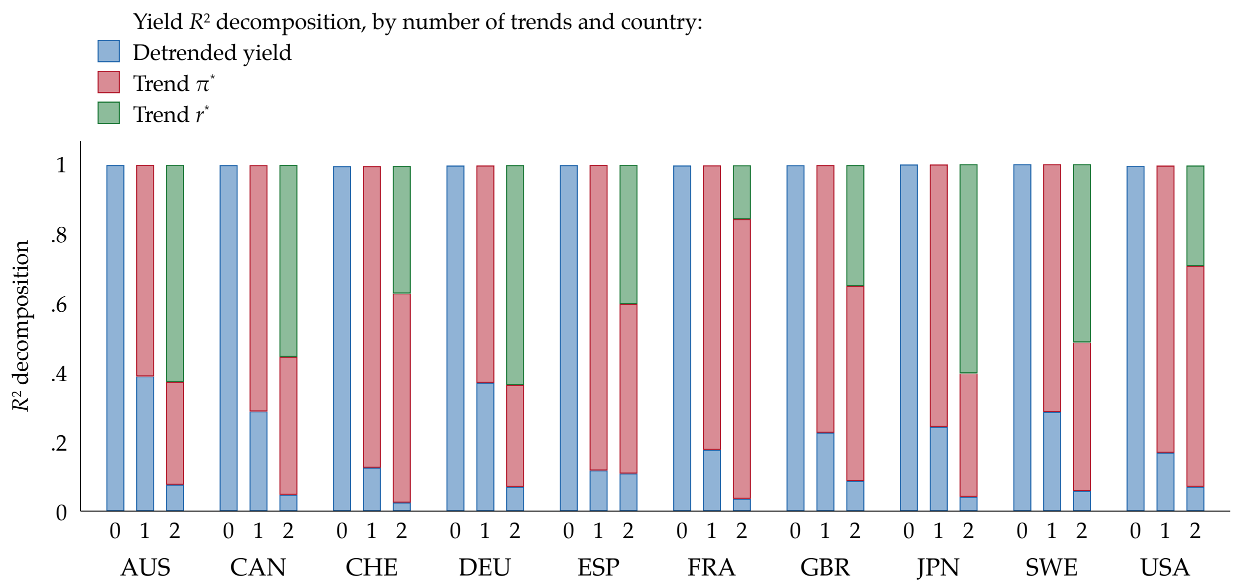

Figure 5: *Decomposition of in-sample fit: excess return regressions with 0, 1, and 2 macro trends*

The chart displays R^2 values for the excess returns regressions by country. 0 denotes the model with no trend, 1 the model with π^* trend, and 2 the model with π^* and r^* trends.

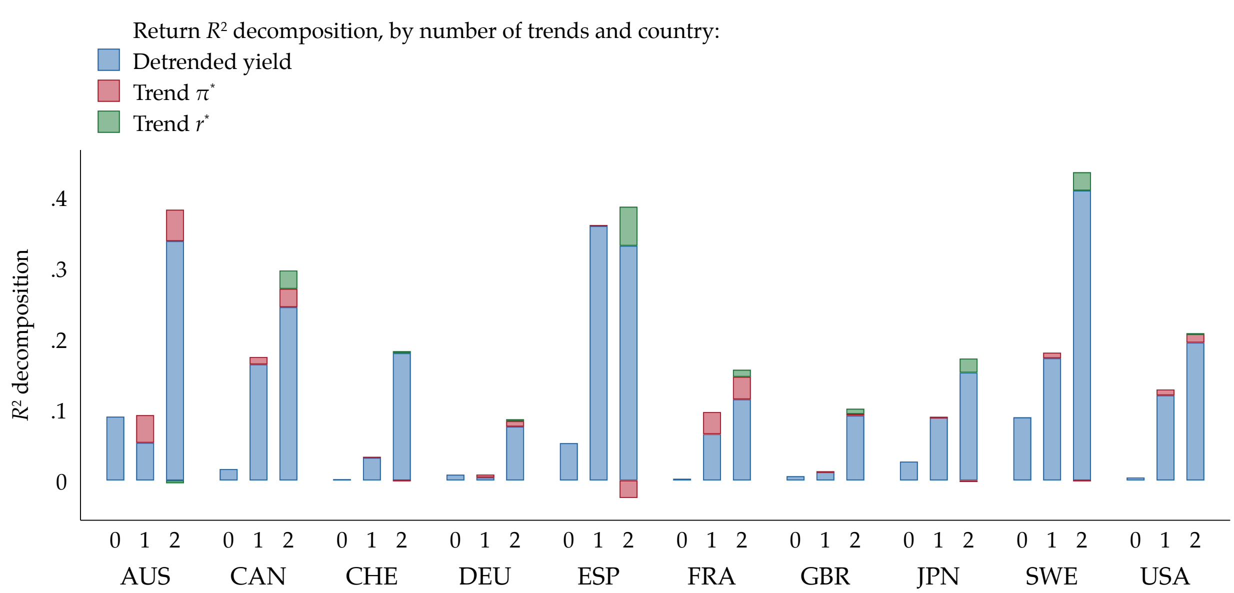

Figure 6: *In- versus out-of-sample performance: MSE ratio evaluation for the 2010s period*

For this chart, model residuals are collected for all ten countries in each period, and the resulting mean squared error, *MSE*, is calculated. The null model is the 0-trend model with only a yield factor $\bar{y}$. *MSE* ratio for other models is shown relative to the null. The alternative models add: (I) 1-trend using π^*; (II) 1-trend using r^*; and (III) 2-trends using π^* and r^*.

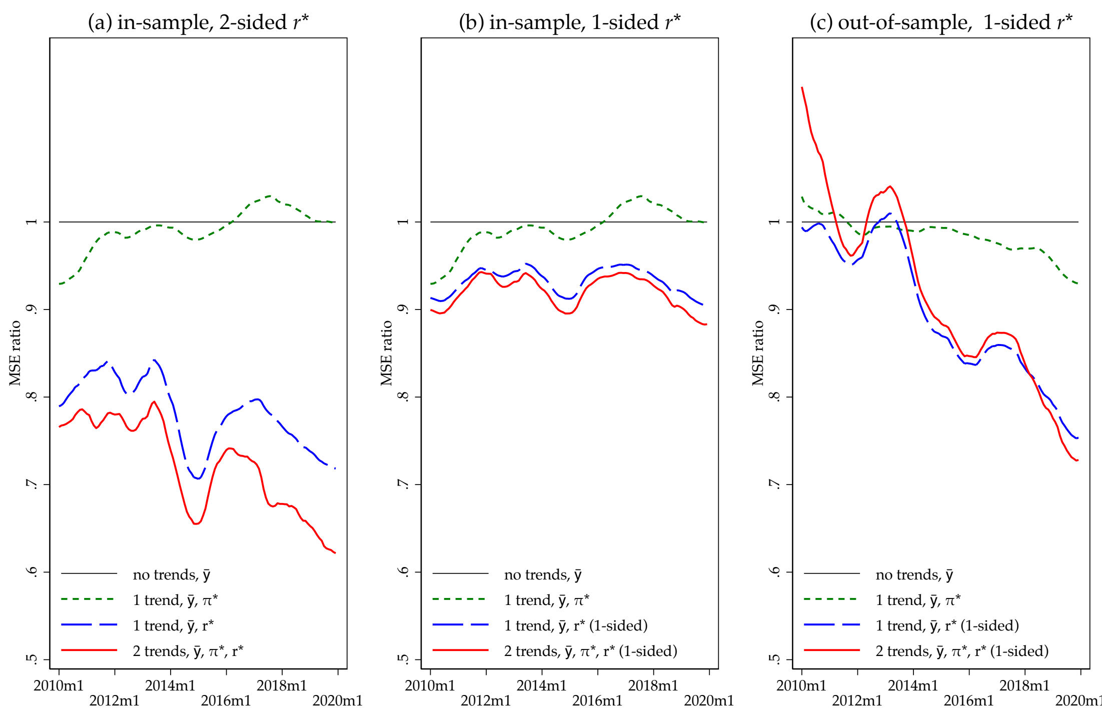

First, Panel (a) reports findings using in-sample estimates and the 2-sided Kalman Filter estimates of the natural rate. As might be expected, the best performing models were II and III, since movements in the natural rate were more salient in this period than changes in inflation. MSE ratios of 0.7 are achieved relative to the null. Next, Panel (b) reports findings using in-sample estimates and the 1-sided Kalman Filter estimates of the natural rate. The same ranking of model performance is seen again, but now the performance gains are reduced since future information is not being used in any period by the filter, and MSE ratios of 0.9 are achieved relative to the null. Finally, Panel (c) reports findings using out-of-sample estimates with an expanding window and the 1-sided Kalman Filter estimates of the natural rate. Here again, accruing over time we see significant improvement of models II and III over the null model, and model I. MSE ratios of 0.7 are achieved relative to the null by the end of the window.

The final results here confirm that the 2-trend model also improves out-of-sample fit in a meaningful way, so that the extension from a 0-trend or 1-trend model is delivering true performance gains in real time.

7. Assessing the natural rate trends in 10 advanced economies

We now turn to a discussion of the plausibility of our model estimates of the natural rate, the latent r^* time series which we obtain for all 10 countries. Associated with this natural rate trend, we can also plot the values of trend growth g, and the headwinds term z, where $r^* = g + z$, by definition, which can give further insight into the interpretation of the trends.

These estimates are displayed in Figure 7. Again we stress that prior work has not been able to generate a natural rate estimate for as many countries over as long a period in the postwar period, but we can still discuss the relevance and plausibility of these estimates as compared to prior consensus views and also by direct comparisons in places of overlap with other estimates in Figure 8 and Figure 9.

In this section we now discuss these comparisons, before moving on to evaluate how well our estimates conform with the drivers most commonly associated with the decline in r^*, namely slowing economic growth and demographic aging.

Overview The top panel in Figure 7 shows the natural rate estimates, and we can make several remarks here. First, the natural rate has in general been falling over time for all countries, although not monotonically, and some reversals are larger than others. This finding is consistent with previous historical works documenting the long-run decline of real rates over the long to very-long run (Jordà, Knoll, Kuvshinov, Schularick, and Taylor, 2019; Rogoff, Rossi, and Schmelzing, 2022). As recently as the 1990s, natural rates in these countries were between 100 and 600 bps. At the end of the sample 8 out of 10 countries have a negative r^*, and the other 2 are between 0 and 50 bps.

Taking a closer look at the evolution across time in natural rates, we do however see a general shift upwards across all countries in the 1960s–1980s period, even if the timing varies from one country to the next. And perhaps the most dramatic coherence across countries is seen in the sharp downward trend in r^* that is set in motion around the year 2000. This was previously noted for one or two countries, starting with the U.S., and various explanations have been offered for that phenomenon, including not just slower growth but also demographics, the EM savings glut, the falling price of investment, among others (Rachel and Smith, 2017; Del Negro, Giannone, Giannoni, and Tambalotti, 2017; Rachel and Summers, 2019; Cesa-Bianchi, Harrison, and Sajedi, 2022). What we see here is how broadly that phenomenon was experienced across a wide swath of advanced economies.

Lastly, we see that the dispersion of natural rates across countries also falls over time At the start of each country's sample period, in the 1970s and 1980s, the natural rate estimates range widely between about 100 and 800 bps. But by the end of the sample in all 10 countries have a natural rate sit in a narrower interval between –100 and 50 bps. This would be consistent, mechanically, with convergence in either the g or z terms — which we discuss in a moment — and also aligns with the idea that under common forces (of demography or via globalization in technology or finance), in the long run, countries may be under the sway of a common global factor in r^* (Clarida, 2019).

Figure 7: *Trends in r^*, g, and z in international data, our estimates*

The top chart displays our estimates of the natural rate r^*, the middle chart trend growth g, and the bottom chart the estimates of the headwinds term z, where $r^* = g + z$, by definition.

(a) Trends in r^*

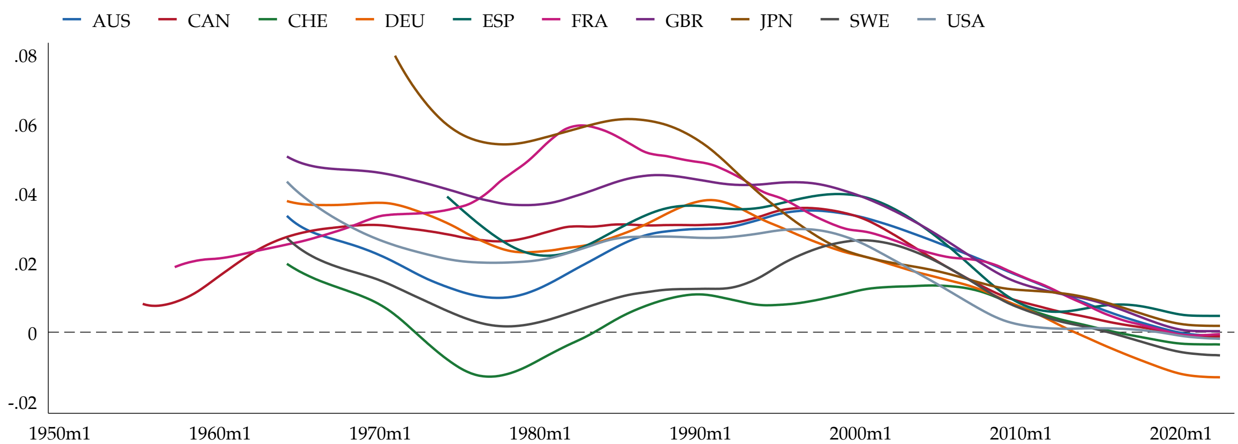

(b) Trends in g

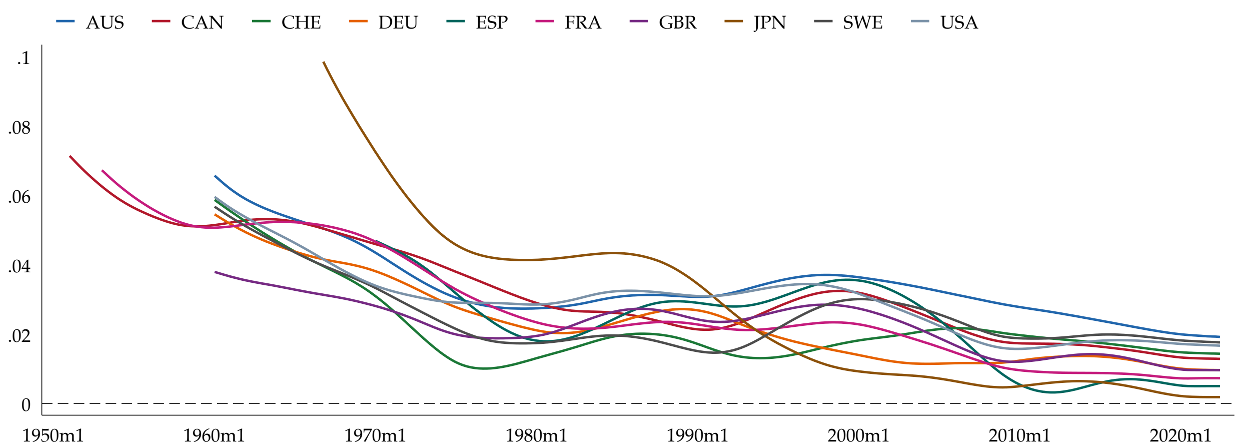

(c) Trends in z

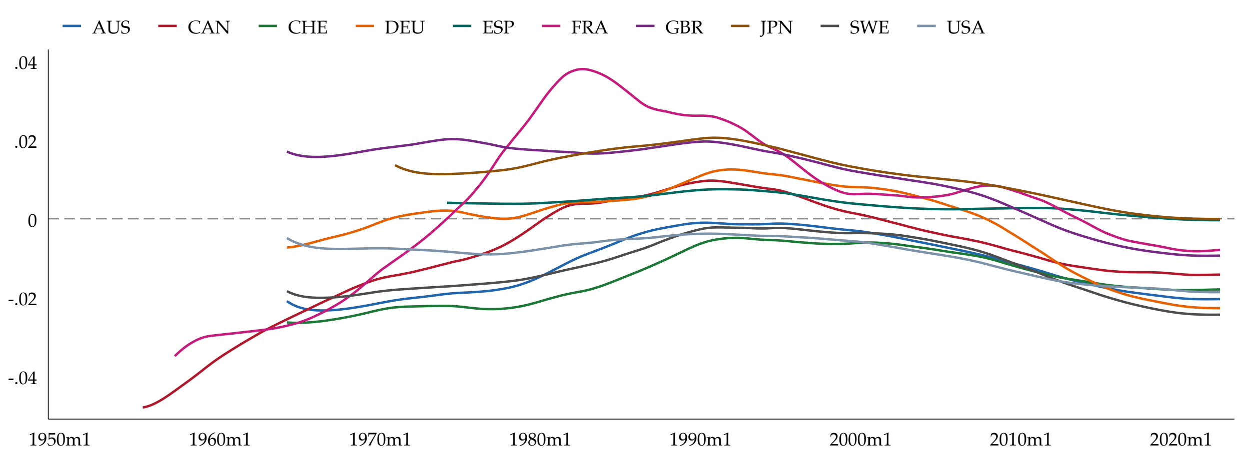

Figure 8: *Trends in r^*, our estimates versus HLW*

The charts display the four HLW estimates of the natural rate r^* and our 2-sided estimates.

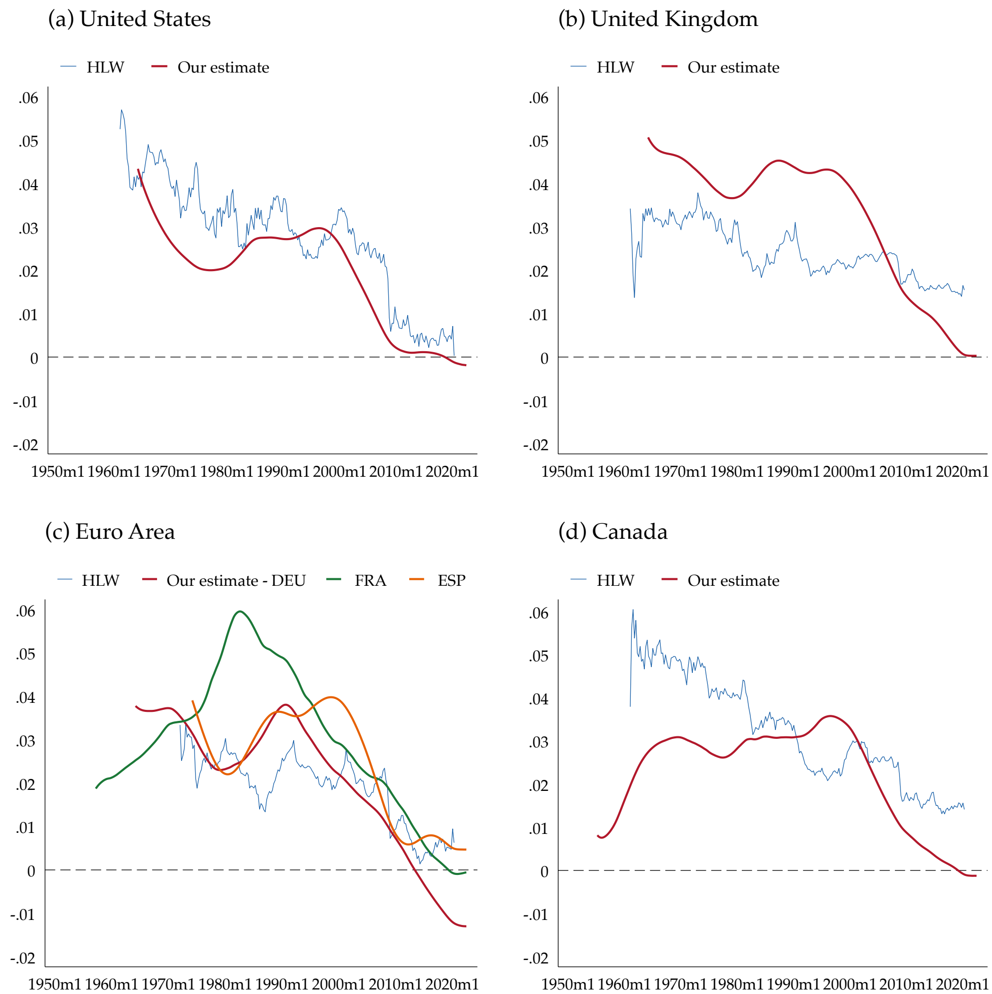

The middle panel in Figure 7 shows the evolution of growth rates g. We can see two immediate implications from this chart. First, in line with common wisdom, trend growth rates have been declining inexorably during the postwar decades, with rare reversals. They have also tended to converge, but started to do so earlier than any convergence in natural rates. Thus, whilst some of the variation in the country-level natural rates r^* across space and time can be explained by g, this is by no means the entire story and so much work is left for the residual.

The final panel in Figure 7 shows the important role played by the non-growth headwinds term z in accounting for variations across time and space in natural rates. Most striking here is the rise in this z term, often more than offsetting the decline in growth g during the 1970–1990 period, which is why natural rates tended to rise in that time frame. In contrast, the z term reaches a synchronized peak around 1990, and then enters a secular decline in all countries. This captures a global bond

Figure 9: *Trends in r^*, our estimates versus other estimates*

The charts display various estimates of the natural rate r^* and our estimates. Our estimates are shown in both 2-sided (solid line) and 1-sided (dashed line) forms. Other estimates are shown as a scatter using the following abbreviations in the legends: GJST = Grimm, Jordà, Schularick, and Taylor (2023); DGGT = Del Negro, Giannone, Giannoni, and Tambalotti (2017) for USA and Del Negro, Giannone, Giannoni, and Tambalotti (2019) for others; HLW = Holston, Laubach, and Williams (2017); LM = Lubik and Matthes (2015); BOJ = Okazaki and Sudo (2018); RBA = McCririck and Rees (2017).

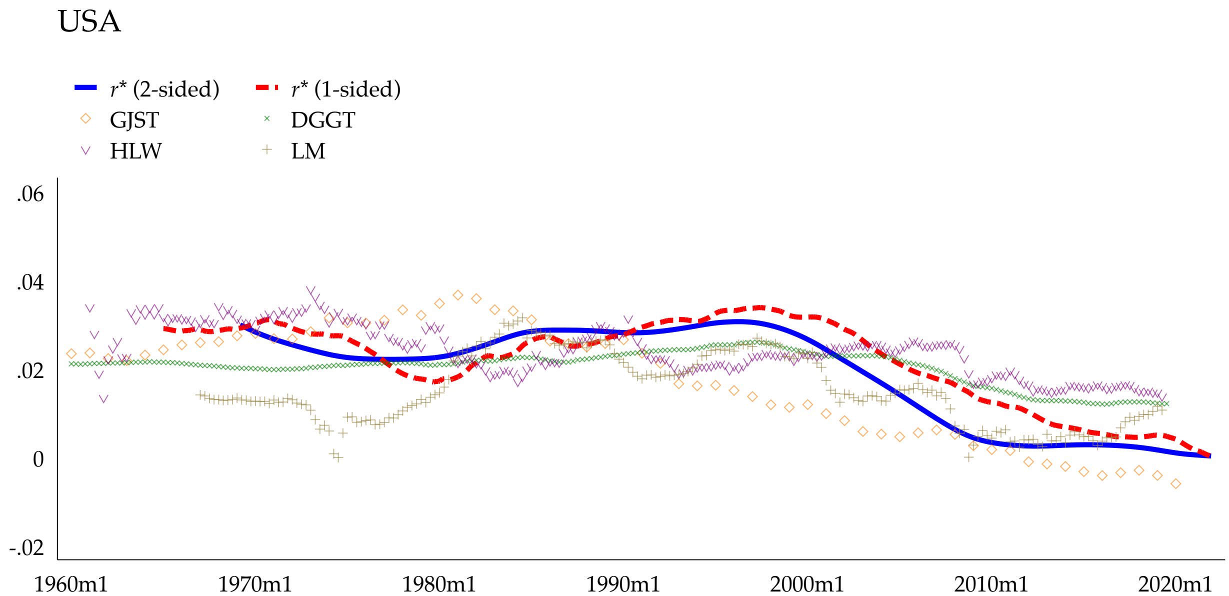

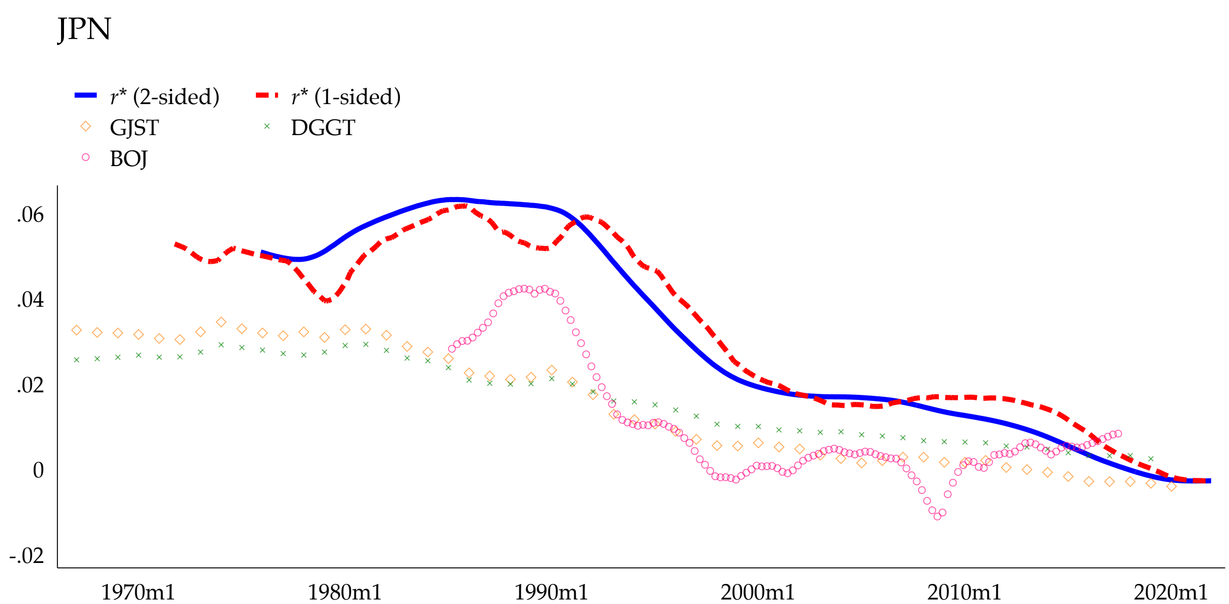

Figure 9: *Trends in r^*, our estimates versus other estimates (continued)*

DEU

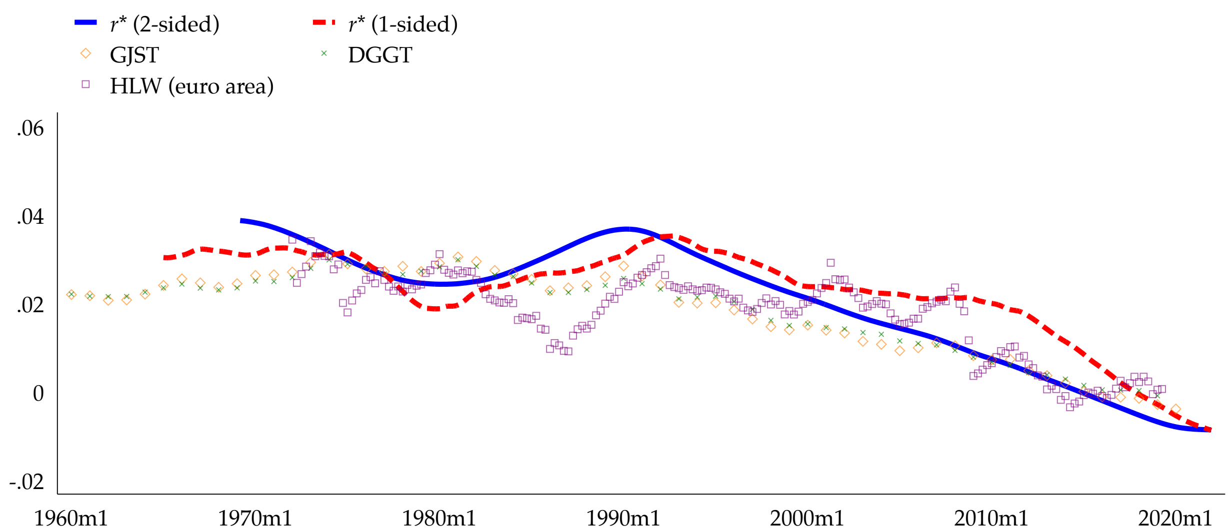

GBR

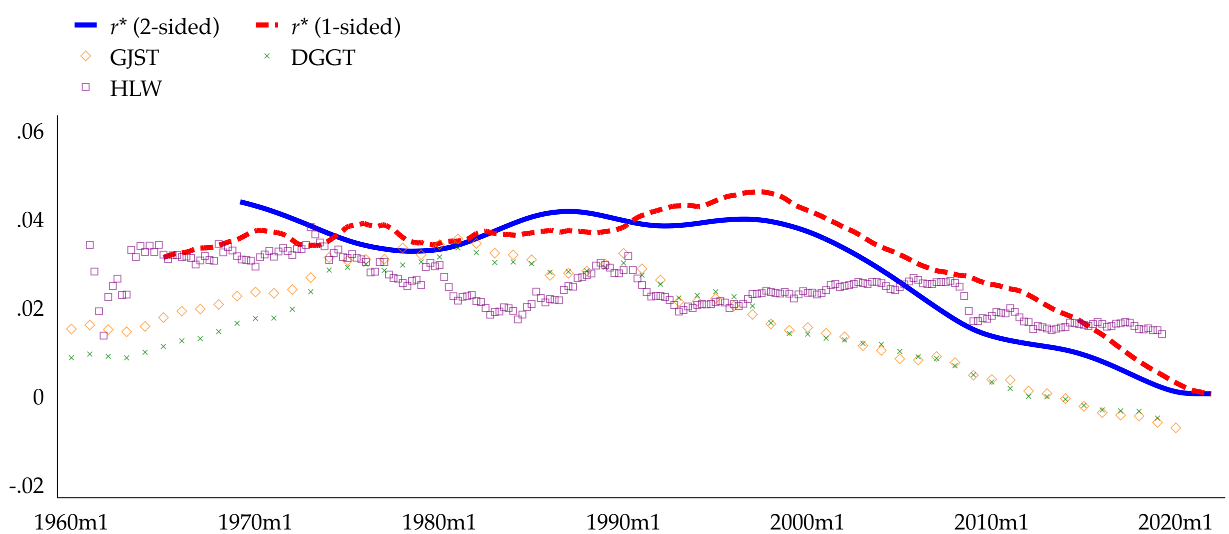

Figure 9: *Trends in r^*, our estimates versus other estimates (continued)*

AUS

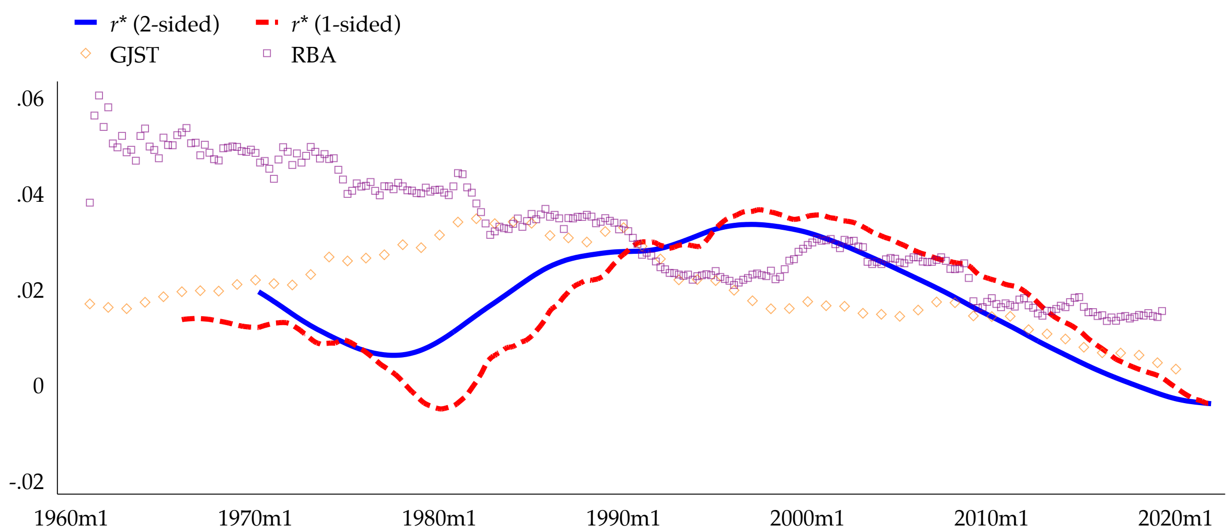

CAN

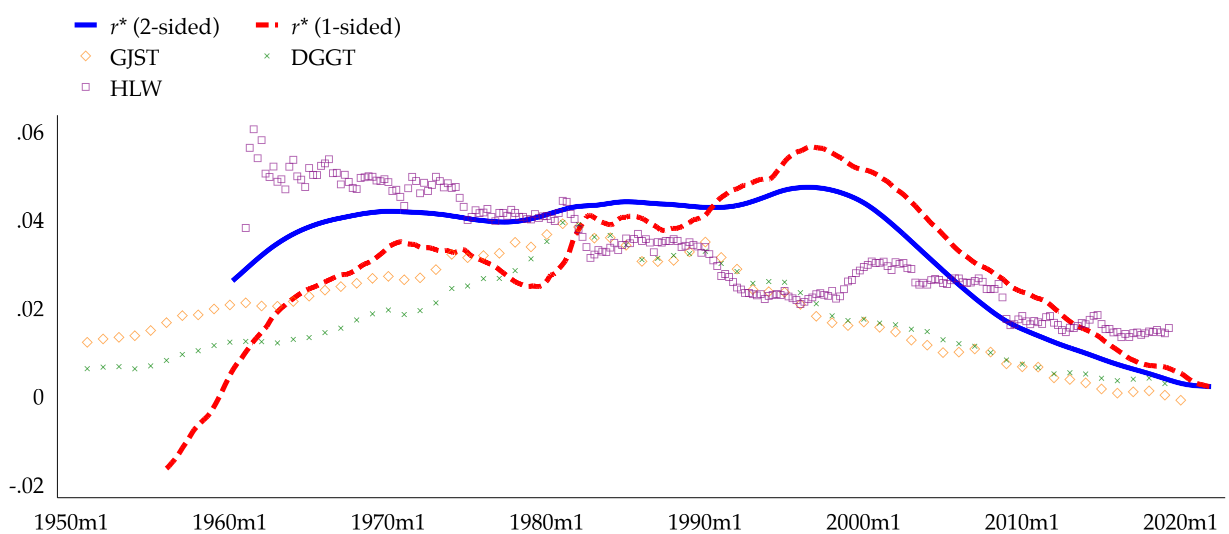

Figure 9: *Trends in r^*, our estimates versus other estimates (continued)*

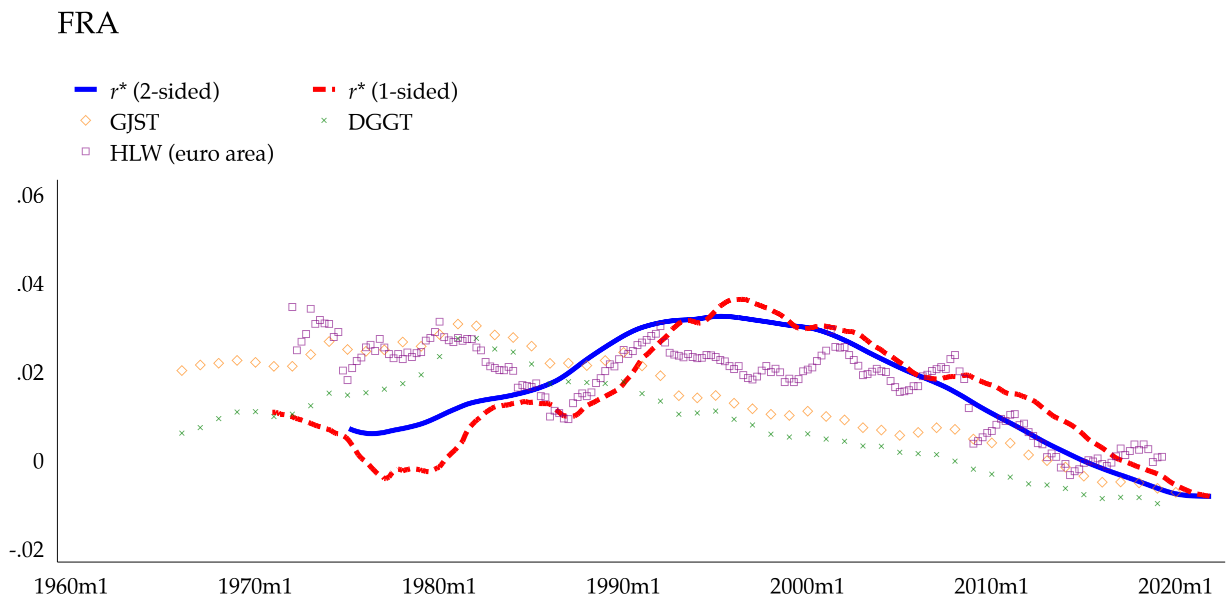

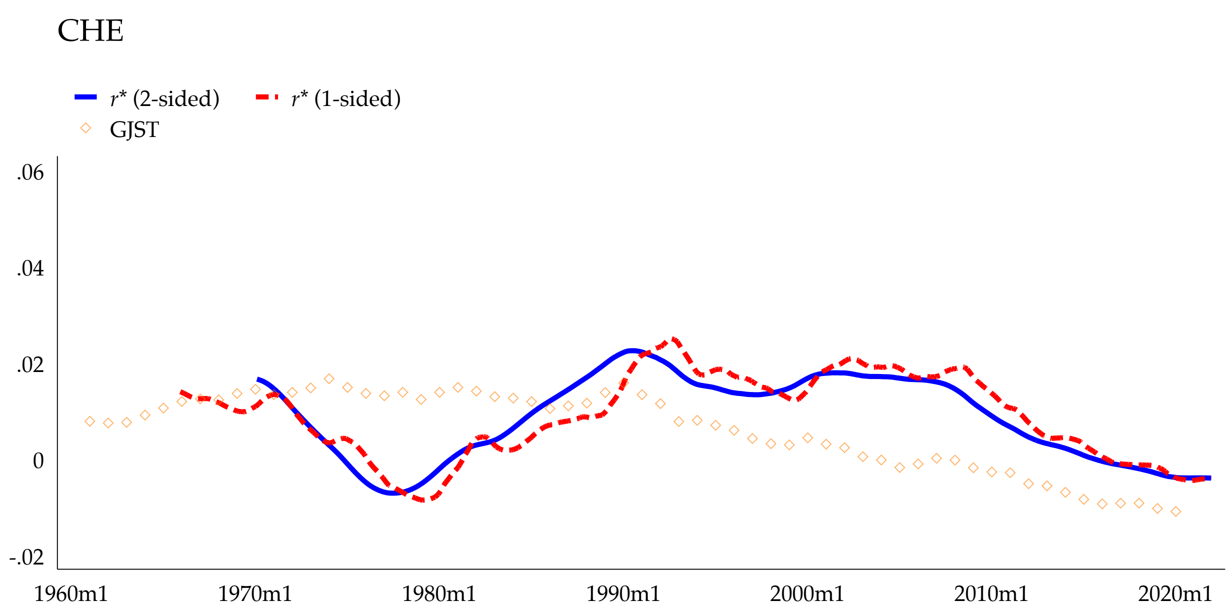

Figure 9: *Trends in r*, our estimates versus other estimates (continued)*

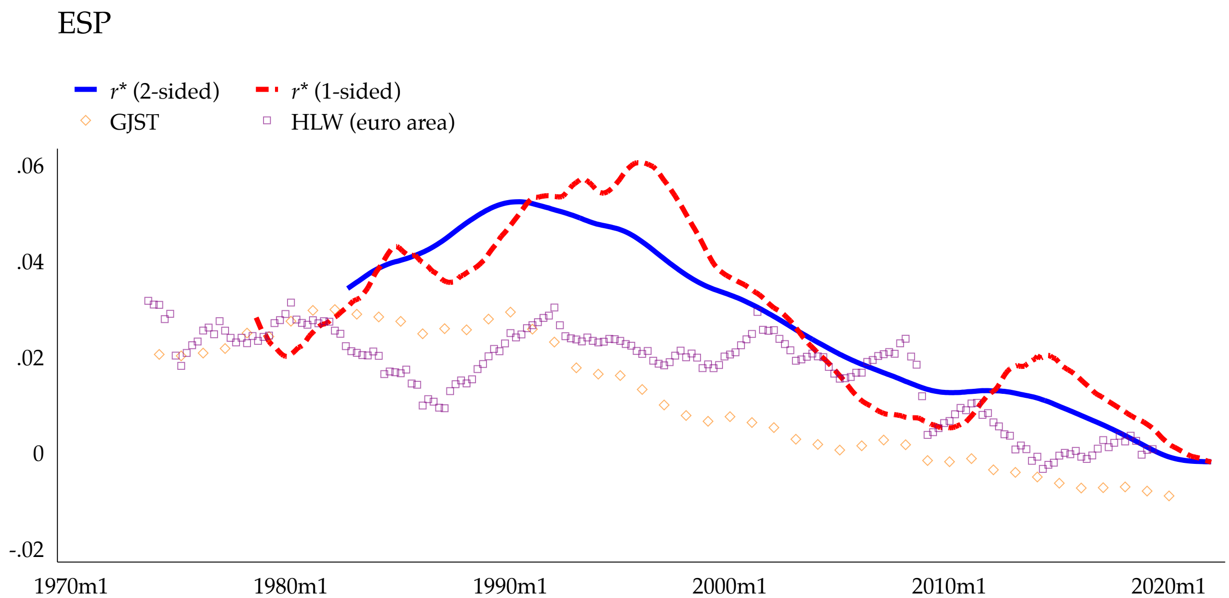

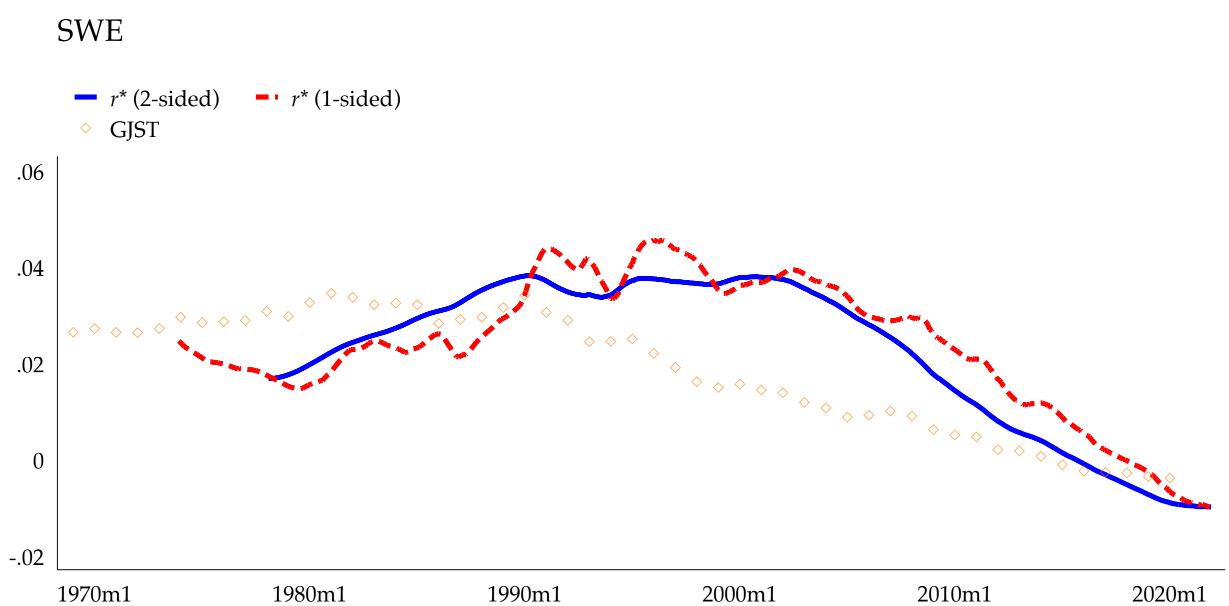

market "conundrum" — to use Greenspan's term — whereby the decline in real rates in the last thirty years takes on a pronounced turn beyond what can be explained by growth fundamentals alone. Seen here, the extra headwinds in the form of a fall in z were experienced not just in the U.S. but across all advanced economies, consistent with trends, like demographics and investment prices, that were witnessed in all of these countries.

Comparison with HLW and other estimates As we have noted before, for cross-country estimates, Holston, Laubach, and Williams (2017) [HLW] is the earliest, best-known, and most widely-used precursor of our work, a study which provided natural rate estimates for 4 countries. So as a first sense check we compare our natural rate estimates to HLW for the U.S., U.K., Canada, and the Euro Area (which we compare to our series for Germany, France, and Spain).

In Figure 8 we see that our U.S. natural rate series is close the the HLW series in shape but is in general at a much lower level. In the 1970s and again in the 2000s, our series is about 100–200 bps lower and towards the end of the sample we find a negative natural rate when the HLW series is still positive. In the Euro Area, our series shows more of a rise and fall pattern, and generally finds a much steeper decline after the 1990s, with natural rates turning negative in France and especially Germany. For the U.K., we see an upswing and very large downswing in natural rates in the 1990s and afterwards, and the natural rate drops to zero at the end, about 200 bps below the HLW estimate. A similar decline is seen for the case of Canada, as well as much lower natural rates earlier in the sample. We surmise that our estimates differ from the HLW because we are using information from the bond market at the longer end curve (via $\bar{y}$), so our somewhat different trends may arise because of substantial variations in the headwinds component z could become apparent in longer-maturity bonds, with larger shifts in average yields than are implied from a model linked to GDP growth and short rates alone.

In Figure 9 we take comparisons much further and utilize all of the current natural rate estimates that we could find for all 10 of the countries in our sample. From this exercise we conclude that our estimates are not wildly out of line with previous work, but there are some notable difference in amplitude and timing. The other estimates are, in addition to HLW, as follows:

- GJST = Grimm, Jordà, Schularick, and Taylor (2023) for all 10 countries;
- DGGT = Del Negro, Giannone, Giannoni, and Tambalotti (2017) for USA and Del Negro, Giannone, Giannoni, and Tambalotti (2019) for 6 others;
- LM = Lubik and Matthes (2015) for USA;
- BOJ = Okazaki and Sudo (2018) for JPN; and
- RBA = McCririck and Rees (2017) for AUS.

In general, our estimates suggest that the decline in natural rates over the last 50 years has been somewhat larger in terms amplitude and somewhat later in terms of timing, as compared to other estimates. In almost all cases, we find the sharpest declines do not really commence until around the 1995–2005 window, with the exception of Japan where as is well understood, the downswing had begun much earlier. In Europe, the trends in Germany and Spain begin the decline earlier than others, but for other European countries the main shift starts a bit later, and the peak is maybe even later still in Britain and the three New World economies.

The global and local components of natural rates For further insight into the global pattern of natural rates over time we do a mechanical decomposition into global and local components. Let r^*_{Wt} denote the cross sectional average $\frac{1}{N}\sum_i r^*_{it}$ in period t of our natural rate estimates in $N = 10$ countries.

Then,

$$r^*_{it} = \underbrace{r^*_{Wt}}_{\text{global component}} + \underbrace{r^*_{it} - r^*_{Wt}}_{\text{local component}}$$

and again we can use the Fields (2003) regression decomposition method for R^2 to attribute contributions of explanatory power to each term. For clarity, we do this exercise decade by decade. And since R^2 is one we opt to scale by the standard deviation of r^*_{it}, so that contributions to the amplitude of natural rates can be compared over time in absolute terms.

The results shown in Figure 10 are striking. From the 1970s to the 1990s, variations in natural rates were dominated by local rather than global factors, and in absolute terms they were large. In the 2000s and 2010s, variations were perhaps one-half due to global factors, but in absolute terms they were smaller.

Figure 10: *Decomposition of r^*: local versus global components*

The chart displays the Fields (2003) regression decomposition of natural rates decade by decade, scaled by the standard deviation of r^*_{it}. See text.

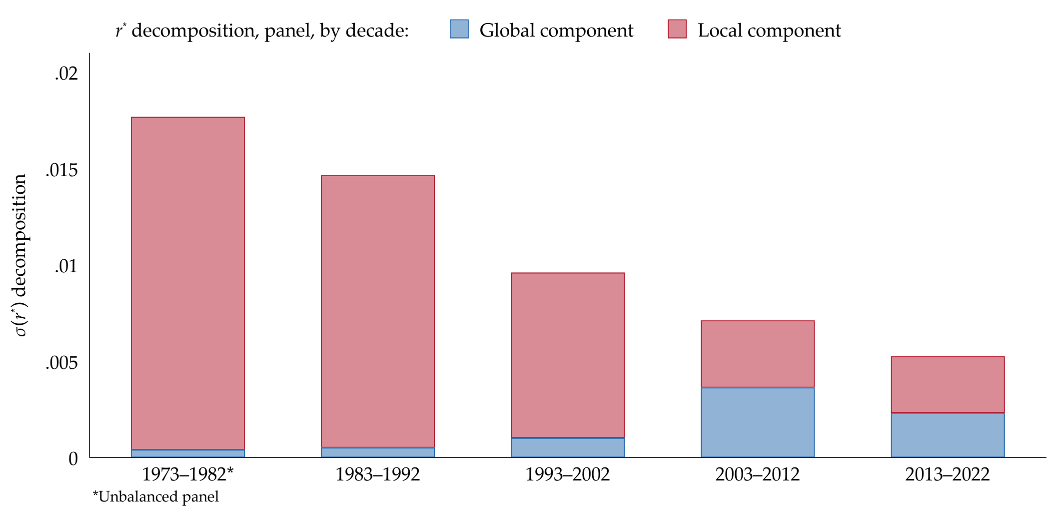

We think this aligns with intuition, both in terms of the likely deep drivers of natural rates, and also the scope for global arbitrage. Before the 1990s, countries were hit by more idiosyncratic growth shocks and were also in different demographic trajectories. As we show later, empirically, as well as theoretically, these drivers matter for r^*. But after the 1990s all advanced countries followed more similar trajectories of low growth and aging demographics. In addition, financial globalization was weak before the 1990s, so the extent to which capital could flow, and interest rates could be arbitraged, as limited. Both explanations would lead us to expect larger differences in natural rates further back in time.

8. Major drivers of natural rates: growth and demography

In a final exercise we explore whether our new natural rate estimates are consistent with some of the prevailing explanations in the literature for the secular decline of natural rates over recent decades. The two drivers we focus on are the rate of growth and demography, since these have been found to be consistent and dominant forces in many studies that have examined recent real rate trends (Carvalho, Ferrero, and Nechio, 2016; Rachel and Smith, 2017; Rachel and Summers, 2019; Eggertsson, Mehrotra, and Robbins, 2019; Cesa-Bianchi, Harrison, and Sajedi, 2022; Kopecky and Taylor, 2022) The literature has used a variety of calibrated equilibrium models (PE and GE) as well as reduced-form saving-investment models, to argue for the importance of these channels. But given the extent of our new natural rate estimates for 10 countries over many decades, we explore the question with a direct panel econometric approach.

Panel estimating equation We suppose the headwinds term z depends on growth g, demography summarized by the age structure $\boldsymbol{D}$, and other factors $\boldsymbol{X}$, so that $r* = g + z = f(g, \boldsymbol{D}; \boldsymbol{X})$. We will assume growth affects r^* linearly as ϕg , but not necessarily with a unit coefficient, since theory is ambivalent on this point. In a standard neoclassical model, as noted, the coefficient $c = 1/\sigma$ depends on the EIS parameter; but in life-cycle OLG models, growth can affect aggregate saving, since, all else equal, slower (higher) growth implies a need to save (borrow) more for smoothing, since less (more) future income will materialize; conversely, buffer-stock motives may work in the opposite direction; on the investment side, all else equal, lower growth entails less investment demand. Overall, higher growth g may be associated with higher natural rates, with $\phi > 0$ as saving supply falls and investment demand rises. As for the demography channel, an OLG model with variable income and labor participation across ages will also generate aggregate saving that depends on the population age shares, with young-adults saving little, or borrowing, middle-age adults saving a lot, and the older workers and retirees holding on to their wealth to provide retirement income in a world of stochastic mortality and, possibly, also bequest motives. On the investment side, we also expect more workers (non-workers) to be associated with higher (lower) investment demand.[10]

[10]Various works have examined demographic impacts on consumption, saving and investment quantities. See, e.g., Aksoy, Basso, Smith, and Grasl (2019) and Kopecky (2023).

These modeling assumptions align with the standard intuition that, all else equal, the age structure $\boldsymbol{D}$ will have an inverted-U shaped relationship with r^*, with net positive effects from younger-age lower-wealth people in work, and net negative effect from older higher-wealth people near to or in retirement. As we see below, this intuition is consistent with the empirical evidence.

We want to estimate the empirical relationship between growth, population structure, and r^*. A saturated approach would be to estimate a panel country fixed-effects model

$$r^*_{it} = a_i + \phi g_{it} + \sum_{j=1}^{J} \alpha_j p_{j,it} + \theta \boldsymbol{X}_{it} + \epsilon_{it} , \tag{33}$$

where $p_{j,it}$ is the population age share in bin j, in country i, at time t, and wlog the α_j sum to one.

For parsimony, and to avoid overfitting to a large number of age shares, we follow Kopecky and Taylor (2022) and fit a Fair and Dominguez (1991) cubic polynomial function to a finite set of age bins $j = 1, \ldots, J$, with $J = 12$, with α_j are fit with a polynomial $\alpha_j = \gamma_0 + \gamma_1 j + \gamma_2 j^2 + \gamma_3 j^3$, with γ_0 obtained from the restriction that the α_j sum to one.

We then define

$$D_{1,it} = \left(\sum_{j=1}^{J} j\, p_{j,it} - \frac{1}{J} \sum_{j=1}^{J} j \right) , \; D_{2,it} = \left(\sum_{j=1}^{J} j^2\, p_{j,it} - \frac{1}{J} \sum_{j=1}^{J} j^2 \right) , \; D_{3,it} = \left(\sum_{j=1}^{J} j^3\, p_{j,it} - \frac{1}{J} \sum_{j=1}^{J} j^3 \right) . \tag{34}$$

An equivalent linear estimating equation, absorbing all other factors $\boldsymbol{X}$ into the error term, is then

$$r^*_{it} = a_i + \phi g_{it} + \sum_{k=1}^{3} \gamma_k D_{k,it} + \epsilon_{it} , \tag{35}$$

and estimates of the α_j terms can be recovered from the estimated γ_k.

Model estimates, drivers and predictions To estimate this equation we take our annual natural rate estimates r^*_{it} for all 10 countries, along with growth rates g_{it}, over the post-1970 sample and merge them with annual UN population age-structure estimates, as used in Kopecky and Taylor (2022), from which the $D_{1,it}, D_{2,it}, D_{3,it}$ terms can be built. This yields an almost-balanced panel of about 500 observations. The resulting estimates are shown in Table 8 and the implied α_j effects by age bin are shown in Figure 11.

The baseline model in Column (1) fits will with an R^2 of 0.62. A model with quartic and quintic polynomial terms was found to fit no better, as those higher-order terms were not statistically significant, so we stick to the cubic approximation. The cubic term is small and positive, and so in the relevant range the approximation is close to quadratic, but flatter to the right as j increases. The coefficient on growth is positive, as expected, but the effect is less than one-for-one. The age effects follow the expected inverted-U shape, with young adults ages 20–49 having a net positive effect on r^*, but older adults 55+ having a net negative effect. To guard against spurious regression with

Table 8: *Empirical model of natural rates using Fair and Dominguez (1991) age effects specification*

	(1) r^*	(2) r^*
g	0.594***	0.573***
	(0.055)	(0.053)
D_1	0.173129***	0.172479***
	(0.023356)	(0.022492)
D_2	−0.022371***	−0.017606***
	(0.004696)	(0.004581)
D_3	0.000687**	0.000350
	(0.000254)	(0.000250)
Time trend		−0.000384***
		(0.000059)
Constant	0.0334***	0.0424***
	(0.0028)	(0.0030)
N	543	543
R^2	0.674	0.698

Standard errors in parentheses
* $p < 0.05$, ** $p < 0.01$, *** $p < 0.001$

Figure 11: *Implied α_j effects of population share on r^* by age bin*

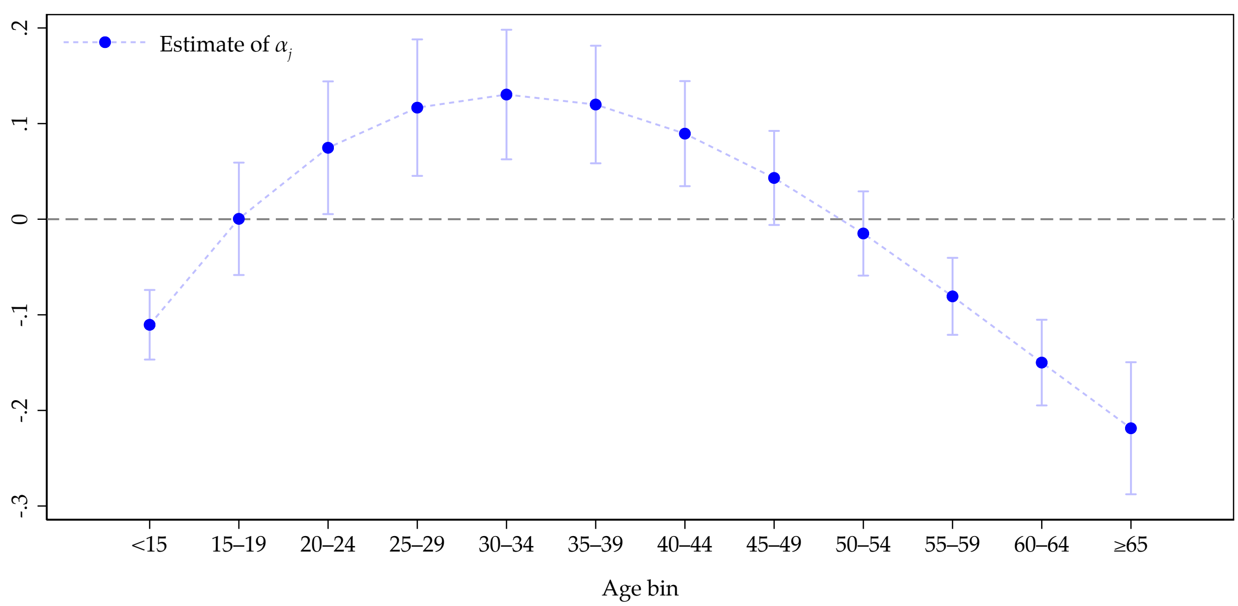

trending variables in Column (2) we also estimated the model with a time trend (year minus 2000) but the results were very similar, with a mild global time trend of minus 3.84 bps per year.

We now want to ask how well this empirical model can fit the observed historical data. The evolution of the right-hand-side variables since 1970 can tell us right away that the model has the potential to work, as is well known. Looking at these underlying drivers in Figure 12 and Figure 13, the patterns are clear and consistent. Over 50 years, the rate of growth in the advanced economies steadily declined, with some cross-sectional timing variation. And, over those same 50 years, the over 55 age-share in the advanced economies steadily rose, again with some timing variation. In both cases, the trends become stronger and more uniform across countries from the 1990s onwards. And in both cases, the trends were most extreme in Japan, as is also well known.

To evaluate the fit, we take the model and compare the actual and fitted values of r^*_{it}. For clarity, we demean by country, and aggregate observations into quinquennial averages. The results are shown as a scatter plot in Figure 14. Here countries move from top right towards bottom left, over time, although some reversals happen along the way as growth and demographic factors fluctuate.

What might be surprising is that the model fit is quite respectable. The correlation of actual and fitted natural rates is about $^2/_3$, as is the slope of the line of best fit for these data ($\beta = 0.66$, as shown). In Japan both the actual and fitted natural rate fell by about 650 bps. The fit is almost exact, and close to the 45-degree line, for the case of Japan, suggesting a close to 100% explanatory power. In other countries the decline is 300 bps or less, and shallower slope allows that other factors may have played a minor contributing part to the decline in r^*.

Thus, in our new and large sample of annual r^* estimates for 10 advanced economies, across time and space we find a strong role for growth and demography as drivers or declining real rates in our empirical model, which serves to corroborate and extend previous theoretical decompositions based on "global" natural rate estimates built for a single group aggregate of advanced economies (cf. Rachel and Summers, 2019; Cesa-Bianchi, Harrison, and Sajedi, 2022).

9. Conclusion: Alternative histories of the global bond market

The finance approach to interest rates uses term-structure models of the yield curve but excludes macro factors. The macro approach to interest rates in the Wicksellian tradition downplays financial market information. Both omit potentially valuable information and lead to a puzzle with contradictory interpretations of recent bond market trends.

We propose a bridge between these approaches and utilize both macro and financial market information in an encompassing model. Returning to the puzzle identified in section 2 via the limiting decomposition equation Equation 1, in Figure 15 we reconsider long run trends in light of our new natural rate estimates. Recalling the notation $f - \pi - r^* = \Gamma$, we plot forward rates (10y-10y), then we subtract inflation and the natural rate to infer the proxy limiting risk premium term, showing all these time series for all 10 countries, along with y, the corresponding nominal 10-year zero coupon yield, which tends to track the forward rate over long periods.

Figure 12: *Trends in g in each country after 1970*

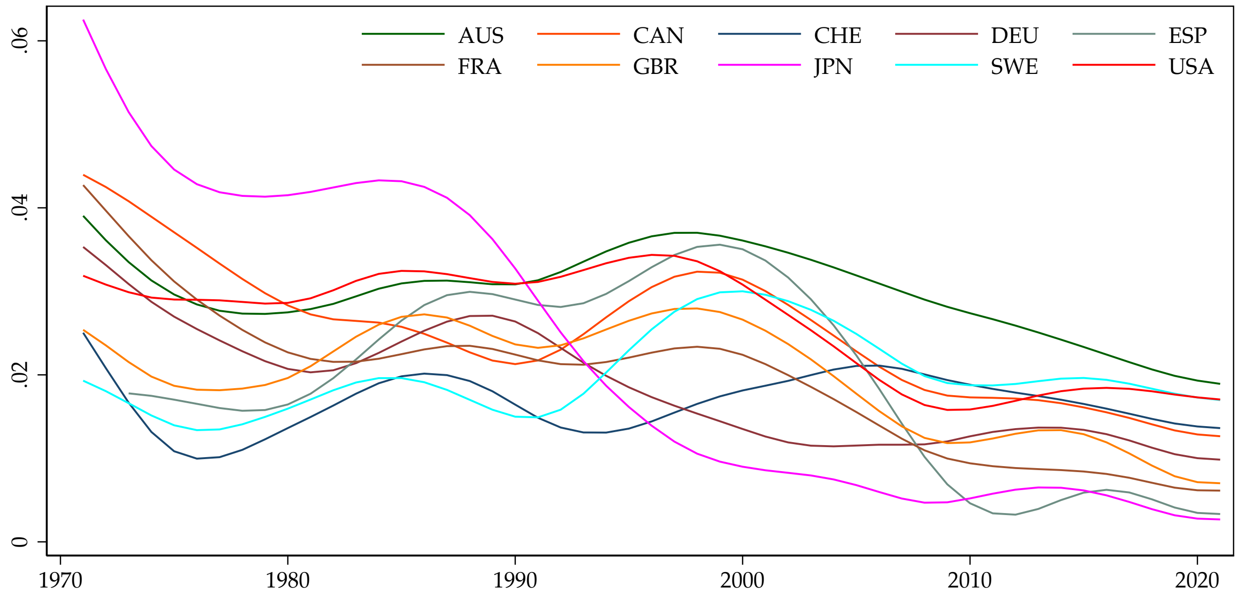

Figure 13: *Trends in the over-55 age share in each country after 1970*

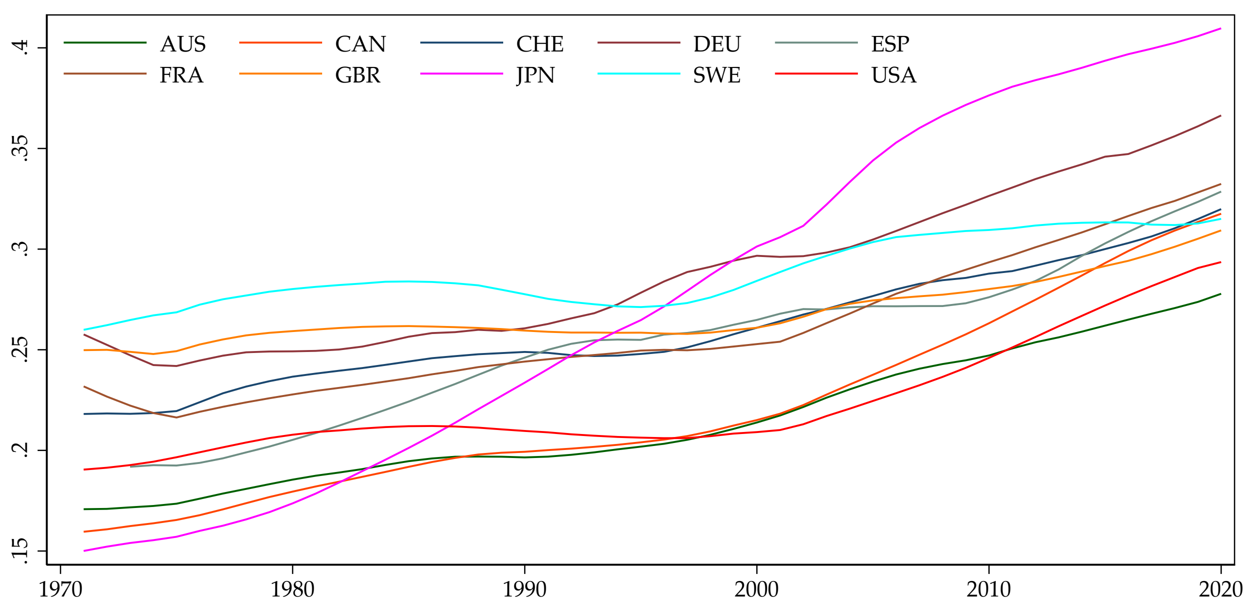

Figure 14: *Actual and fitted natural rates from the empirical model after 1970*

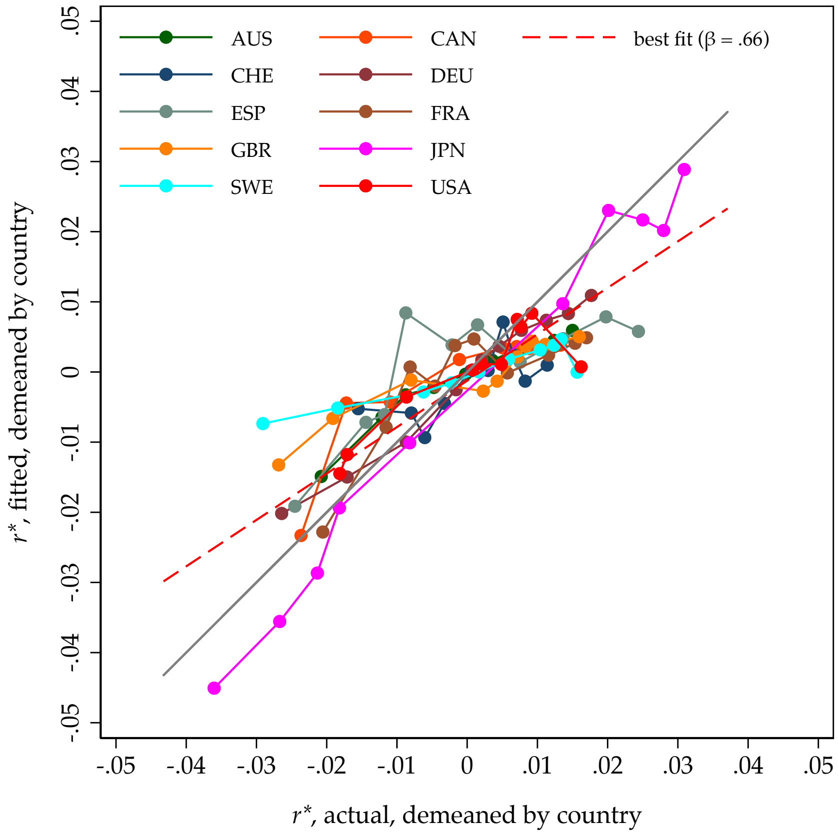

These results point towards a new historical narrative of the bond market over 50+ years that tells a somewhat different story. Take the U.S., where yields have often been seen as being driven by falling inflation and bond risk premia since the peak of inflation circa 1980. But as we saw, that interpretation has rested on finance models of risk premia that exclude macro factors (e.g. Adrian, Crump, and Moench, 2013), and the same issues arise in other countries traditional histories. Yet here, bringing macro factors to the fore, we obtain a picture of mostly flat risk premia over time in the U.S., as seen in the figure, and instead a more dominant role for the downward trend in the natural rate. The same change of story applies in general to the other advanced countries, where allowance for falling natural rates in this decomposition also tends to leave less variation to be accounted for by the residual risk premium proxy: compare the red dashed line ($f - \pi$) and the orange dotted line ($f - \pi - r^* = \Gamma$).

In the process of trend construction, we showed how these findings rest on a macro-finance modeling framework that delivers objective improvements in model performance. Our 2-trend market-implied estimates deliver better yield regression fit and better excess return forecasts than 0- and 1-trend models. This holds in-sample and out-of-sample. These estimates also differ from both

Figure 15: *Resolution of the puzzle: forwards, macro trends, and the residual*

the prior macro and finance approaches, but they resolve the puzzle by coming down closer to the macro view.

Finally, we stress that our natural rate estimates have trends and turning points much like consensus macro estimates, and they tend to converge over time to a common path, but they differ in being typically somewhat lower in the recent years that many other estimates. We find bigger "headwinds" with natural rates converging near zero or even negative in all 10 countries by 2020, intensifying concerns about secular stagnation and proximity to the effective lower-bound on monetary policy in advanced economies. Mapping our estimates of the natural rate into growth and demographic drivers, we find that these two contributing factors can explain most of the decline seen since the 1970s. Going forward, economic and population projections look stable, and forecasts of continued slow growth and further aging in the advanced economies in coming decades would mean that natural rates will remain lower for longer absent any other major shocks.

References

Adrian, Tobias, Richard K. Crump, and Emanuel Moench. 2013. Pricing the term structure with linear regressions. *Journal of Financial Economics* 110(1): 110–138.

Adrian, Tobias, Richard K. Crump, and Emanuel Moench. 2015. Regression-based estimation of dynamic asset pricing models. *Journal of Financial Economics* 118(2): 211–244.

Aksoy, Yunus, Henrique S. Basso, Ron P. Smith, and Tobias Grasl. 2019. Demographic structure and macroeconomic trends. *American Economic Journal: Macroeconomics* 11(1): 193–222.

Ang, Andrew, and Monika Piazzesi. 2003. A no-arbitrage vector autoregression of term structure dynamics with macroeconomic and latent variables. *Journal of Monetary Economics* 50(4): 745–787.

Bauer, Michael D., and Glenn D. Rudebusch. 2017. Interest Rates Under Falling Stars. Working Paper Series 2017-16, Federal Reserve Bank of San Francisco.

Bauer, Michael D., and Glenn D. Rudebusch. 2020. Interest Rates under Falling Stars. *American Economic Review* 110(5): 1316–54.

Bernanke, Ben. 2015. Why are interest rates so low, part 4: Term premiums. Brookings Institution. https://www.brookings.edu/blog/ben-bernanke/2015/04/13/why-are-interest-rates-so-low-part-4-term-premiums/.

Caballero, Ricardo J., Emmanuel Farhi, and Pierre-Olivier Gourinchas. 2008. An Equilibrium Model of "Global Imbalances" and Low Interest Rates. *American Economic Review* 98(1): 358–93.

Cadorel, Jean-Laurent. 2022. The French Historical Yield Curve Since 1870. Paris School of Economics. Unpublished.

Campbell, John Y., and Robert J. Shiller. 1987. Cointegration and Tests of Present Value Models. *Journal of Political Economy* 95(5): 1062–1088.

Carvalho, Carlos, Andrea Ferrero, and Fernanda Nechio. 2016. Demographics and real interest rates: Inspecting the mechanism. *European Economic Review* 88: 208–226. SI: The Post-Crisis Slump.

Cesa-Bianchi, Ambrogio, Richard Harrison, and Rana Sajedi. 2022. Decomposing the drivers of Global R*. Bank of England Working Paper 990.

Cieslak, Anna, and Pavol Povala. 2015. Expected returns in Treasury bonds. *Review of Financial Studies* 28(10): 2859–2901.

Clarida, Richard H. 2019. The Global Factor in Neutral Policy Rates: Some Implications for Exchange Rates, Monetary Policy, and Policy Coordination. International Finance Discussion Papers 1244, Board of Governors of the Federal Reserve System.

Cochrane, John H., and Monika Piazzesi. 2005. Bond risk premia. *American Economic Review* 95(1): 138–160.

Del Negro, Marco, Domenico Giannone, Marc P. Giannoni, and Andrea Tambalotti. 2017. Safety, Liquidity, and the Natural Rate of Interest. *Brookings Papers on Economic Activity* 48(1): 235–316.

Del Negro, Marco, Domenico Giannone, Marc P. Giannoni, and Andrea Tambalotti. 2019. Global trends in interest rates. *Journal of International Economics* 118(C): 248–262.

Duffee, Gregory. 2013. Forecasting Interest Rates. In *Handbook of Economic Forecasting*, edited by Graham Elliott, Allan Timmermann, volume 2, chapter 7, 385–426. Amsterdam: North-Holland.

Duffee, Gregory R. 2011. Information in (and not in) the Term Structure. *The Review of Financial Studies* 24(9): 2895–2934.

Duffie, Darrell, and Rui Kan. 1996. A yield-factor model of interest rates. *Mathematical finance* 6(4): 379–406.

Eggertsson, Gauti B., Neil R. Mehrotra, and Jacob A. Robbins. 2019. A Model of Secular Stagnation: Theory and Quantitative Evaluation. *American Economic Journal: Macroeconomics* 11(1): 1–48.

Fair, Ray C., and Kathryn M. Dominguez. 1991. Effects of the Changing U.S. Age Distribution on Macroeconomic Equations. *American Economic Review* 81(5): 1276–1294.

Fields, Gary S. 2003. Accounting for Income Inequality and its Change: A New Method, with Application to the Distribution of Earnings in the United States. In *Worker Well-Being and Public Policy*, volume 22 of *Research in Labor Economics*, 1–38. Bingley: Emerald Group.

Grimm, Maximilian, Òscar Jordà, Moritz Schularick, and Alan M Taylor. 2023. Loose Monetary Policy and Financial Instability. NBER Working Paper 30958.

Grishchenko, Olesya V., Franck Moraux, and Olga Pakulyak. 2020. Fuel up with OATmeals! The case of the French nominal yield curve. *Journal of Finance and Data Science* 6: 49–85.

Gürkaynak, Refet S., Brian Sack, and Jonathan H. Wright. 2007. The US Treasury yield curve: 1961 to the present. *Journal of Monetary Economics* 54(8): 2291–2304.

Holston, Kathryn, Thomas Laubach, and John C. Williams. 2017. Measuring the natural rate of interest: International trends and determinants. *Journal of International Economics* 108: S59–S75. 39th Annual NBER International Seminar on Macroeconomics.

Jordà, Òscar, Katharina Knoll, Dmitry Kuvshinov, Moritz Schularick, and Alan M Taylor. 2019. The Rate of Return on Everything, 1870–2015. *Quarterly Journal of Economics* 134(3): 1225–1298.

Jordà, Òscar, and Alan M. Taylor. 2019. Riders on the Storm. In *Challenges for Monetary Policy*, Proceedings of a symposium sponsored by the Federal Reserve Bank of Kansas City, Jackson Hole, Wyo., August 23–24, 2019, 17–59. Kansas City, Mo.: Federal Reserve Bank of Kansas City.

Joslin, Scott, Kenneth J. Singleton, and Haoxiang Zhu. 2011. A New Perspective on Gaussian Dynamic Term Structure Models. *Review of Financial Studies* 24(3): 926–970.

Kim, Don H., and Jonathan H. Wright. 2005. An arbitrage-free three-factor term structure model and the recent behavior of long-term yields and distant-horizon forward rates. Finance and Economics Discussion Series 2005-33, Board of Governors of the Federal Reserve System.

Kopecky, Joseph. 2023. Population age structure and secular stagnation: Evidence from long run data. *Journal of the Economics of Ageing* 24: 100442.

Kopecky, Joseph, and Alan M. Taylor. 2022. The Savings Glut of the Old: Population Aging, the Risk Premium, and the Murder-Suicide of the Rentier. NBER Working Paper 29944.

Kozicki, Sharon, and P. A. Tinsley. 2001. Shifting endpoints in the term structure of interest rates. *Journal of Monetary Economics* 47(3): 613–652.

Laubach, Thomas, and John C. Williams. 2003. Measuring the natural rate of interest. *Review of Economics and Statistics* 85(4): 1063–1070.

Litterman, Robert B., and José Scheinkman. 1991. Common Factors Affecting Bond Returns. *Journal of Fixed Income* 1(1): 54–61.

Lubik, Thomas A., and Christian Matthes. 2015. Time-Varying Parameter Vector Autoregressions: Specification, Estimation, and an Application. *Federal Reserve Bank of Richmond Economic Quarterly* (4Q): 323–352.

Ludvigson, Sydney C., and Serena Ng. 2009. Macro factors in bond risk premia. *Review of Financial Studies* 22(12): 5027–5067.

McCririck, Rachael, and Daniel Rees. 2017. The Neutral Interest Rate. *RBA Bulletin* (September): 9–18.

Nelson, Charles, and Andrew F. Siegel. 1987. Parsimonious Modeling of Yield Curves. *Journal of Business* 60(4): 473–89.

Okazaki, Yosuke, and Nao Sudo. 2018. Natural Rate of Interest in Japan: Measuring its size and identifying drivers based on a DSGE model. Working Paper Series 18-E-6, Bank of Japan.

Piazzesi, Monika. 2010. Affine Term Structure Models. In *Handbook of Financial Econometrics: Tools and Techniques*, edited by Aït-Sahalia, Yacine, and Lars Peter Hansen, volume 1 of *Handbooks in Finance*, chapter 12, 691–766. Amsterdam: North-Holland.

Rachel, Lukasz, and Thomas D. Smith. 2017. Are Low Real Interest Rates Here to Stay? *International Journal of Central Banking* 13(3): 1–42.

Rachel, Łukasz, and Lawrence H. Summers. 2019. On Secular Stagnation in the Industrialized World. *Brookings Papers on Economic Activity* (Spring): 1–54.

Rogoff, Kenneth S., Barbara Rossi, and Paul Schmelzing. 2022. Long-Run Trends in Long-Maturity Real Rates 1311–2021. NBER Working Paper 30475.

Summers, Lawrence H. 2015. Have we Entered an Age of Secular Stagnation? *IMF Economic Review* 63(1): 277–280.

Svensson, Lars E. O. 1994. Estimating and Interpreting Forward Interest Rates: Sweden 1992–1994. NBER Working Paper 4871.

Wright, Jonathan H. 2011. Term Premia and Inflation Uncertainty: Empirical Evidence from an International Panel Dataset. *American Economic Review* 101(4): 1514–34.

A. Appendix

Bayesian estimation of the state-space model

We estimate the model using Bayesian inference. First, Bayesian methods are a potent framework to handle latent variables in state-space models as the one presented here. Second, it allows us the use prior distributions to regularize the estimation of the unobserved low-frequency macroeconomic and high-frequency financial drivers in the model. In particular, it allows us to impose priors that ensure that the headwinds factor, z_{t+1}, captures structural macroeconomic phenomena.

Bayesian inference constructs a posterior distribution $p(\theta|Y)$ by combining a likelihood $p(Y|\theta)$ and prior distribution $p(\theta)$ as follows

$$p(\theta|Y) = \frac{p(Y|\theta)p(\theta)}{p(Y)} \tag{36}$$

where Y is the set of observations, and the marginal data density $p(Y)$ is a normalization constant independent of the estimated parameters θ. Since we cannot easily compute moments of the posterior $p(\theta|Y)$ or directly sample from it, we use a random-walk Metropolis-Hastings (RWMH) algorithm, a Markov chain Monte Carlo (MCMC) method, to sample from the posterior $p(\theta|Y)$.

We then estimate the state-space model using the RWMH algorithm for each country separately. The algorithm builds a Markov chain of posterior draws $\{\theta_n\}_{n=0}^{N}$ which give rise to a sequence of posterior distributions $\{p_n(\theta|Y)\}_{n=0}^{N}$, with the last draw in the sequence being equal to the posterior distribution. At each step n, the algorithm propagates the parameter vector, or the particles θ_{n-1}, such that over the whole sequence, the parameter vector $\{\theta_n\}_{n=0}^{N}$ represents the target distribution $p(\theta|Y)$. Thus, at each step n, the algorithm draws a new proposal particle ϑ_n, conditional on the previous particle θ_{n-1}, the set of observations Y, and the proposal density $q(\cdot|\cdot)$. We accept step n draw ϑ_n with probability

$$\alpha\left(\vartheta_n|\theta_{n-1}\right) = \min\left\{\frac{p(Y|\vartheta_n)p(\vartheta_n)/q(\vartheta_n|\theta_{n-1})}{p(Y|\theta_{n-1})p(\theta_{n-1})/q(\theta_{n-1}|\vartheta_n)}\right\}, \tag{37}$$

where the step n likelihood function $p(Y|\vartheta_n)$ is computed using the Kalman filter on the state-space representation of the model determined by equations Equation 30 and Equation 31. The RWMH algorithm sets the proposal distribution to

$$q\left(\cdot|\theta_{n-1}\right) = N\left(\theta_{n-1}|\mathfrak{c}\cdot\widehat{\Sigma}\right). \tag{38}$$

Formally, the algorithm proceeds as follows

1. **Initialization:** The initial particles are drawn from the prior distribution $\theta_0 \sim p(\theta)$.
2. **Recursive updates:** For $n = 1, ..., N$ recursively update the particle sequence
   (a) Draw step n proposal particles ϑ_n from $q\left(\vartheta_n|\theta_{n-1}\right)$
   (b) Accept new draw with probability $\alpha\left(\vartheta_n|\theta_{n-1}\right)$
   (c) Update the particle sequence: If accepted $\theta_n = \vartheta_n$, else $\theta_n = \theta_{n-1}$
3. Remove the burn-in samples and construct posterior estimates as follows

$$\bar{h} = \frac{1}{N}\sum_{n=1}^{N} h(\theta_n)$$

$\widehat{\Sigma}$ is estimated as the diagonal matrix with entries calculated from the empirical variance of the drawn parameters for the first 1000 draws. We set the constant $\mathfrak{c} = 0.075$ to target an acceptance rate of 23.4 percent, as it is the standard for the optimal acceptance target in Metropolis algorithms.

Our estimation is calculated with a number of simulations equal to 50,000, and assumes the same prior distribution for all countries. We run our RWMH in four parallel chains, which gives us a total of 200,000 iterations for the posterior distribution estimation. Using the posterior mean of the obtained particle sequence as the estimator for the parameter vector θ, we rerun the state-space model to construct our results. However, we also experimented with using the median and mode which did not affect the results.

For each country, we use as input information the inflation expectations measure π_t^* and the real GDP series. We obtain the trend GDP series by applying the HP filter over quarterly GDP data with a smoothing parameter equal to $25,600 = 1600 \cdot 16$. The series thus obtained is interpolated to monthly data, and the trend growth rate g_t is then calculated. Since a filter applied over the entire history of the series would contain forward-looking bias, we have been careful to recalculate the HP filter only with as-of-date information, allowing for the effect of late release in GDP data (that is, we do not assume that GDP figures are available at the end of the corresponding quarter, but at the usual dates at the end of January, April, July and October).

Our identification assumption is r^* cointegrates with the trend GDP series, and that the difference has mean reversion properties compatible with a half-life within business cycle frequency, and not higher. This avoids the problem of r^* acting as a residual term that would capture high-frequency oscillations in bond markets.

Prior specification

We specify tight priors for the parameters of the headwinds factor z_t, and relatively loose priors for other parameters in the model, as detailed in Table A.1. As described above, this way we impose the conjecture that the headwinds factor captures structural macroeconomic phenomena with a frequency similar to that of macroeconomic series. The prior distribution is common for all countries, except for the the headwinds prior volatility σ_z which we set as outlined below.

- The persistence parameter ρ_z is chosen to be close to unit root, but within the unitary circle to prevent an explosive solution. Its magnitude is taken to match a half life of around 60 months. This keeps the headwinds factor within business-cycle frequency and not higher. In a freer setting, this term would act as a residual in the Kalman system and would tend to capture high-frequency variations that are hard to identify given the data.

- The volatility of the headwinds factor σ_z is set to match a relatively small range of variation for the frequency of the headwinds factors. For each country, the prior volatility is chosen based on the relative yield and GDP volatility of the respective country in order to normalize the range of variation in the headwinds frequency. While the drawing process allows for certain range around the 60 months business-cycle frequency, it imposes the view that this variable should not deviate largely from that horizon. Similarly, we impose relatively tight priors on σ_y.

- The model coefficients b_{r^*}, a_y, and b_π are set to have large variances with coefficients centered around values that calibrate the U.S. experience relatively well in a simple regression context.

Table A.1: *Prior specification for model parameters*

Parameter	Distribution	Mean	Variance
ρ_z	Beta	0.997	2.00×10^{-6}
ρ_y	Normal	0.9	0.025
σ_z	Log-Normal	$\bar{\sigma}_z\times10^{-4}$	1.00×10^{-5}
σ_y	Log-Normal	1.00×10^{-3}	5.00×10^{-4}
a_y	Normal	0.00	7.50×10^{-4}
b_π	Normal	1.25	0.10
b_{r^*}	Normal	0.50	0.05

Note: Here $\bar{\sigma}_z$ is a country-specific normalization as we have described. See text.